Study on Forming DNA-Mediated Nanoparticle Conjugates: Toward Detection of COVID-19

By

Chinmay Nitin Afzulpurkar

Presented to the Faculty of the Graduate School of

The University of Texas at Arlington

in Partial Fulfillment of the requirements for the degree of MASTER OF SCIENCE

THE UNIVERSITY OF TEXAS AT ARLINGTON

December 2021

Acknowledgment

I want to thank my Supervising Professor, Dr. Seong Jin Koh, for providing me with this research opportunity and guiding me at every step in my research. Writing this thesis could not have been possible without his guidance, advice, and feedback. I would also like to thank my committee members, Dr. Yum and Dr. Cao, for giving their valuable time to my thesis. I want to thank my group members Pushkar, Anthony, Ojas, Jacob, Mileend, Nnaemeka, and Abdul, for their feedback, support, and help with my research experiments throughout my project and like to extend my thanks to Dr. Hozabari and Nanofab Staff - Dennis, Kevin, and Mick for being so helpful and training me to use the various tools in the Nanofab Research Centre.

I am immensely grateful to my parents, brother, family, and close friends for the invaluable support and motivation throughout my academic journey.

This work was supported by the National Science Foundation (ECCS-2031770 and DMR-2122128).

Abstract

The objective of this thesis is to establish a rapid, robust, and reproducible procedure to controllably assemble DNA-functionalized Au nanoparticles (AuNPs) into satellite-shaped nanostructures using sequence-specific DNA hybridization. A target DNA strand with COVID-19 sequence (t-DNA) is used as a bridge to connect a capture DNA functionalized on a 50nm gold nanoparticle (*C*-AuNP) and a probe DNA functionalized on a 30nm nanoparticle (*P*-AuNP), creating *C*-AuNP/t-DNA/*P*-AuNP conjugates. The *C*-DNA is complementary to a portion of t-DNA, and *P*-DNA is complementary to the other portion of t-DNA. The parameters that affect the conjugate formation, including hybridization buffer strength, hybridization temperature, and DNA lengths, have been studied to increase the efficiency of the process. It is concluded that the hybridization buffer containing 0.6M NaCl at 50 degrees Celcius consistently formed the nanostructures of *C*-AuNP/t-DNA/*P*-AuNP conjugates. The hybridization time for each of *C*-AuNP/t-DNA and *P*-AuNP/t-DNA hybridization was 10 minutes. The optimum nanosatellite formations were obtained when 50 nm AuNPs were functionalized with a mixture of 48-base *C*-DNA and 18-base spacer DNA and 30 nm AuNPs were functionalized with a mixture of 46-base *P*-DNA and 18-base spacer DNA. This sequence-specific controlled formation of nanosatellite structures can be potentially implemented into many fields, such as detection of DNA and RNA of specific pathogens, food safety, and clinical and forensic research.

Contents

List of Figures

List of tables

Chapter1 Motivation and Outline

Nanostructures can be defined as organized assemblies of nanoscale materials. Extensive research has been conducted to fabricate these nanostructures for microelectronics, nanophotonics, and bio/chemical sensors applications.

Typically these nanostructures are fabricated by using two approaches A) Top-down nanolithography[1, 2] approach, and B) Bottom-Up self-assembly approach[3-5].

The Top-down approach uses nanolithography techniques like electron-beam lithography[1, 2] and focuses ion beam milling[6]. The top-down approach can precisely control the shape, size, and spacing. These methods rely on large and externally controlled machines for creating nanostructures and hence have fundamental size restrictions[7]. The bottom-up approach uses self-assembly techniques to fabricate the nanostructures[8, 9]. The bottom-up approach can enable fabricating well-defined nanostructures of precisely small sizes[10]. The DNA-directed self-assembly of nanostructures is particularly studied and implemented to assemble nanostructures[7, 8] utilizing programable molecular recognition of DNA

This study investigates and establishes a novel and systematic bottom-up process to achieve rapid, robust, and reproducible DNA-directed self-assembly of nanostructures. Nanosatellite structures of gold nanoparticles are assembled by hybridizing two DNA-functionalized nanoparticles of different sizes with target DNA (t-DNA) of a specific sequence.

This new approach can assemble nanostructures using any target sequence in a very short assembly time (tens of minutes), making it a good candidate for DNA/RNA detection of specific pathogens, food safety, and clinical and forensic research.

1.2 Thesis outline

The first chapter in this thesis discusses this research's brief statement, motivation, and how this thesis is being approached.

The second chapter will describe basic knowledge and Concepts used in this thesis and includes all the methodologies and different techniques used during the project. Generally, this chapter deals with most of the relevant background and experimental setups in this experiment.

The third chapter gives detailed information about the experimental procedure from Nanoparticle conjugation to sample Preparation to the systematic method for forming saturated satellite structures. In this chapter, we also have given a list of all the tools and reagents used in this project.

The fourth chapter of this thesis focuses on the parameters tested to make the procedure robust and the outcomes of those changes. This chapter also gives a detailed report of problems that occurred while forming the nanosatellite structures and the solutions found to overcome those issues.

The final chapter of this thesis gives a summary of all the results and discussions done in the previous chapters.

Chapter2 Background

The goal of this thesis is to investigate and establish a novel procedure to form the core satellite structure of DNA functionalized gold nanoparticles. A target DNA strand with COVID-19 sequence (t-DNA) is used as a bridge to connect a capture DNA functionalized on a 50nm gold (*C*-AuNP) nanoparticle and a probe DNA functionalized on a 30nm nanoparticle (*P*-AuNP), creating *C*-AuNP/t-DNA/*P*-AuNP conjugates as shown in schematic 1. In this current chapter of background, we will discuss a few concepts used in this thesis, followed by the understanding of fabrication and characterization techniques used

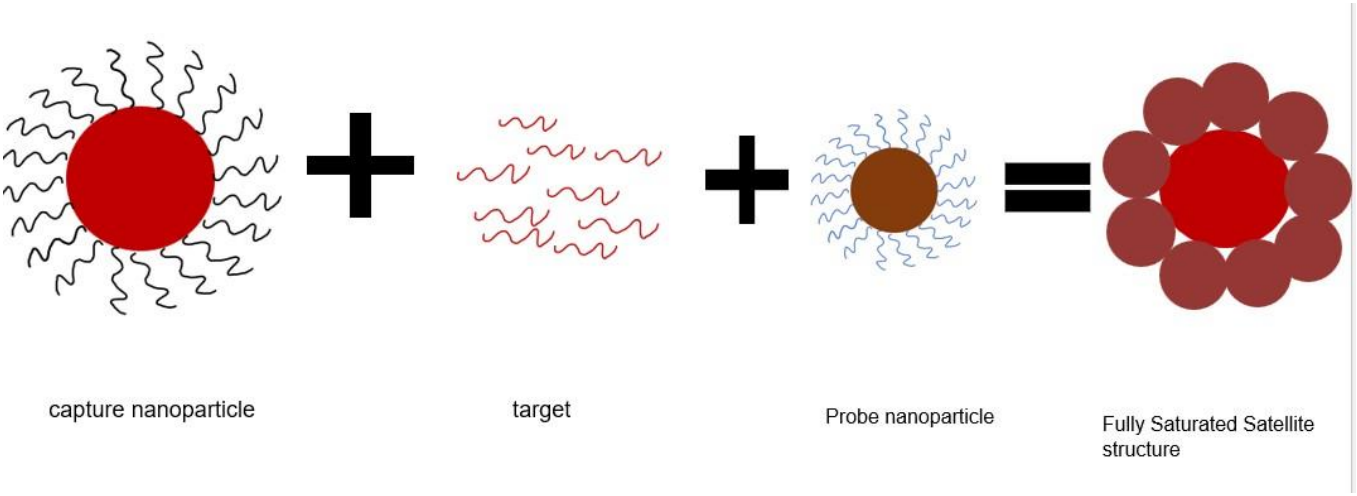

Fig.1: Schematic for satellite structure formation

2.1 DNA Structure

The structure and function of DNA are discussed in this chapter. DNA is the source of all intrinsic genetic information; it plays a crucial role in cells. DNA is a chemically very stable

molecule. Watson and Crick first described the DNA structure in 1953 as a right-handed helix of two individual antiparallel DNA strands[1]. This DNA is made up of a long chain of repeating units called nucleotides. These nucleotides are made up of nucleobase adenine(A), thymine(T), cytosine(C), and guanine(G).[2]

These nucleobases bind together in a specific order via a hydrogen bond. This bonding is called complementary base paring, where Adenine binds with thymine, and guanine bonds with cytosine. The Sugar and Phosphate Group in the DNA acts as a backbone to the helix.

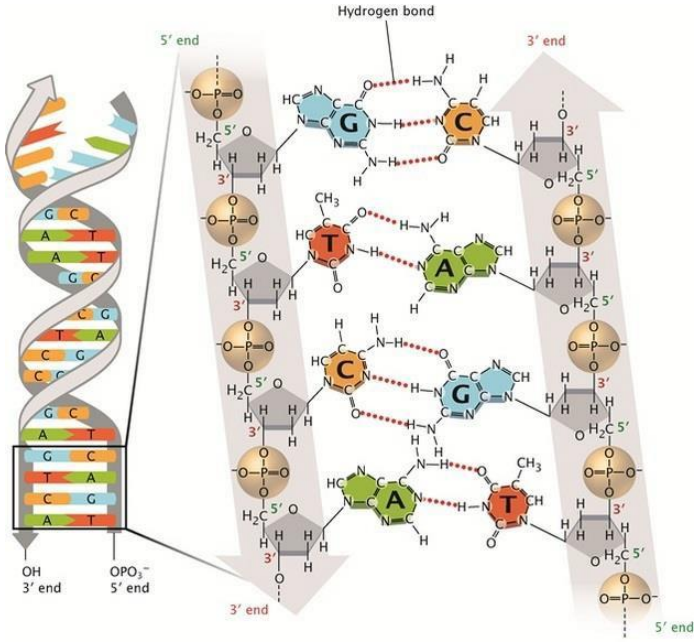

Fig2: Structure of DNA[1]

This double-stranded DNA can be extracted into a single strand by reducing the salt concentration and increasing the temperature. The Phosphate Group carries a negatively charged oxygen making the DNA strand negatively charged.DNA hybridization Is a process in which two complementary nucleobases form a bond to make a double-stranded molecule. [3]

2.2 Nanoparticles

The word Nano in Nanoparticles is a Greek word that means dwarf or extremely small. Nanoparticles are a unique set of materials with a size range of 10nm. These nanoparticles have numerous uncommon chemical and physical properties because of their quantum size and large surface area compared to other metal atoms or bulk metals. Gold nanoparticles (AuNps), in particular very attractive to researchers because of their size and shape-dependent properties[4]

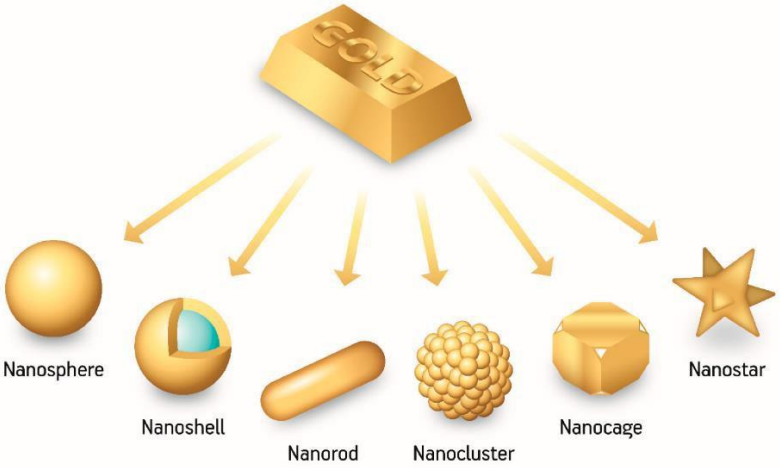

Fig 3 Gold nanoparticles[5]

The Synthesis of these Nanoparticles has always been a research topic with high priority; there are various techniques to synthesize AuNp's like the Chemical method[6], Turkevich method[7], The Brust-Schifrin method [7], Electrochemical method[8], Seeding growth method[9], Biological method[10], Synthesis in ionic liquids [11] and many more techniques

These AuNP's possess unique physical and chemical properties which allows a wide-scale application of these nanoparticles in fields like [12], Biotechnology [13-15], drug delivery[16-19],

Photonics [20-23],Electronics[24-28],Novel sensors[29-32],Biomedicine[33-36] and much more. Few of these properties and nanoparticles' applications have been used in these theses.

2.3 DNA conjugation

Labs of Mirkin and Alivisatos, in 1996, reported a programmable Assembly of DNA-functionalized gold nanoparticles (AuNPs) for the first time [37, 38]. After which many other materials such as quantum dots[39], magnetic nanoparticles[40], silver nanoparticles and other noble nanostructures [41, 42], hydrogels[43], and proteins,[44] have also been functionalized by DNA other than that studies that have already been carried out to functionalize gold electrodes and other bulk gold surfaces with DNA[45, 46]. These DNA-functionalized gold nanoparticles (DNA-AuNPs) have inspired and enabled many aspects of nanobiotechnology ranging from precise Control of interparticle distance[37, 38] directed materials synthesis[47], colorimetric biosensor development[48, 49], and surface-enhanced spectroscopy[50], drug delivery.[51], highly sensitive DNA detection technology and highly efficient gene therapeutics.

Attaching thiolate DNA to AuNPs to achieve a stable conjugate is the first step for all downstream applications. This simple-looking reaction is practically complicated due to negative charge DNA, and Citrate capped AuNPs have a negative surface charge. Due to these negative charges on the surface DNA and nanoparticle, there is a strong repulsion between them.[52] this repulsion can be overcome, and maximum adsorption of DNA on nanoparticles can be achieved by different techniques like The salt-aging method[37, 53, 54], Low Ph method [55, 56] Surfactant-assisted DNA functionalization Using modified DNA Functionalization by depletion stabilization.

Considering all the methods for AuNp DNA conjugation, we devise a systematic method for DNA nanoparticle conjugation.

2.4 Self-assembled monolayers

Self-assembled monolayers are molecules or molecular assemblies formed on a substrate by adsorption [57]. SAM's are made of a head group, a long alkyl chain, and a functional tail group[58], as shown in figure

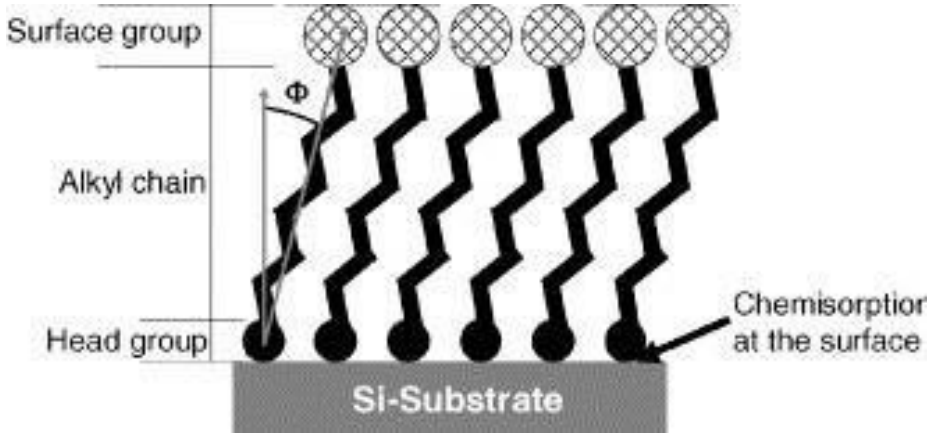

Fig.4 Schematic for self-assembled monolayers [59]

The typical head groups consist of Thiols [60-62], silanes[59, 63, 64], phosphates[65-67]. These head groups have a special affinity for the Substrate and are chemisorbed on the Substrate either from the liquid or vapors phase. This adsorption is a spontaneous process and does not require any special tool or environment. the adsorption of the head group is followed by a slow organization of the tail group and subsequent functional group. The functional group can be modified according to the need. Once the SAM's layer is deposited on the Substrate, it permanently modifies the Substrate.

Due to its easy formation and inexpensive cost, the self-assembled monolayer has wide-scale applications like Control of wetting and adhesion[68], chemical resistance, making bio-compatible sensors[69], nano[70] and microfabrication[59, 71], depositing nanostructures[72].

2.5 Self Assembled Monolayer of APTES

Organic molecules are typically attached to hydroxylated glass or silicon dioxide substrates using alkoxysilanes as coupling agents[70]. 3-aminopropyltriethoxysilane (APTES) is the most popular alkoxysilane coupling agent because of its amine terminations and self-assembly[73]. It allows maximum attachment of organic molecules. APTES is attached to the Silicon surface by salination process where the Substrate is initially hydrolyzed. The APTES ethoxy groups are then hydrolyzed with ethanol as the leaving group, resulting in an aminopropyl-terminated surface. As shown in the figure. These aminopropyl-terminations are facing outward away from the silicon substrate.[74]

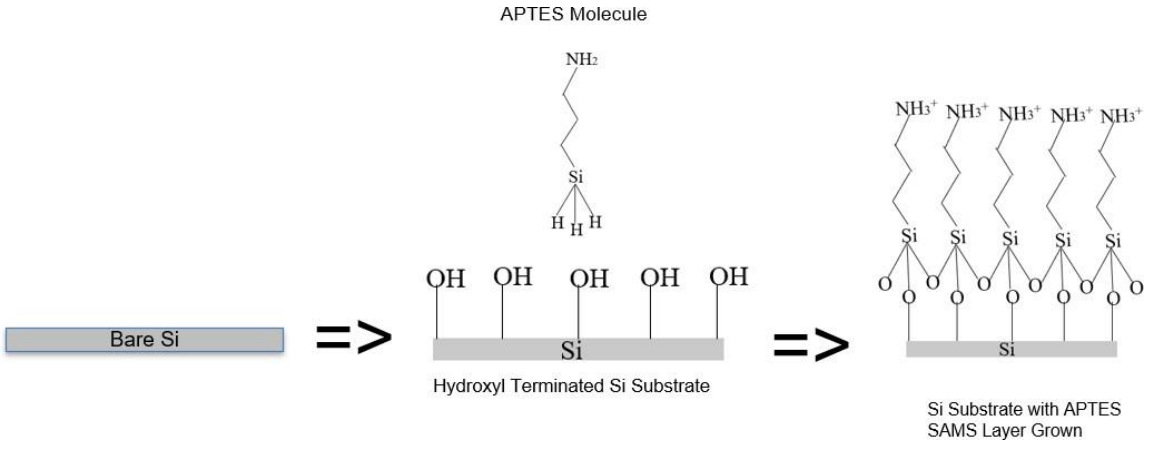

Fig.5

Schematic Representation of APTES formation on Bare Si substrate

Various factors can affect the density, conformation of the covalent bonds of APTES

- Solvent type

When in contact with water, APTES develops zwitterion within itself, and hence an anhydrous solvent is needed to grow APTES SAMs on a substrate[75, 76]. Another issue that can occur due to hydrolysis of the ethoxy group is horizontal polymerization. This can result in Silanol moieties which can further react with each other via condensation reaction creating siloxane bonds[77].

- Time for APTES formation

It is seen that the average density of the APTES coverage continuously increased with increasing reaction time. In an experiment by Vandenberg, a monolayer of APTES was formed, where APTES was deposited in the presence of anhydrous toluene as solvent. The time in the experiment was kept less than 1 hour. In the same experiment, longer salinization time caused polymerization of APTES which caused multilayer formation of APTES or non-uniform coverage on the Substrate [77, 78]

- Drying Process

Work done by Chiang has shown that the air-dried samples with the APTES layer are different from the ones that are Heat cured. For example, the air-dried APTES generally forms one or two siloxane bonds on the surface, whereas Heat cured APTES tends to form three siloxane bonds with the surface[75].

Considering all the points mentioned above, we deposit the APTES SAMs layer on Si substrate. Further, we use APTES to attract functionalized via gold nanoparticles positive charged aminopropyl-terminated group to the damaging charged DNA covered gold nanoparticles. We would further passivate These Amine terminations on the Substrate using Sulfo-SMCC[79]

2.6 Thermal Oxidation

There are various methods to have a stable and uniform layer of Silicone dioxide on a bare Si substrate like Thermal Oxidation[80], Plasma enhanced chemical Deposition[81], Sputtering[82], etc.

From which Thermal oxide produces a uniform and high-density dioxide layer.[83]

The growth of silicon dioxide with the thermal oxidation of single-crystal silicon wafers is a widely used fabrication technique. There are two types of thermal oxidation processes i.e.

a) Wet oxidation wet oxygen (oxygen bubbled through water at 95°C) could be supplied to the quartz oxidation tube.[84]
b) Dry oxidation Either purified or dry oxygen (water content less than5ppm)[85]

With the help of Dry thermal oxide growth, we can produce a highly uniform, high-density with High dielectric strength silicon dioxide layer on top of the standard Substrate.[86] As the thermal oxidation process is quite refined, the growth of the oxide can be precisely controlled with temperature, gas flow, and time. Deal-Grove theory is widely used in the Si oxidation process.[87]We calculate the oxide growth properties by accounting for oxidant diffusion from the oxide layer to the oxide & Si interface and the oxidation reaction at the interface. In the oxidation process, we insert the oxygen atom into the Si-Si bond as we increase the temperature in the

presence of oxygen atoms at the interface. At the interface, as the distance between the Si atom in Si-O-Si is 30% larger compared to Si-Si bonds, this accumulates strain when three oxygen atoms are inserted, which causes the Si-Si bonds to break at the interface, and these Si atoms are emitted from the surface and create a bond with oxygen to form Silicon Dioxide.[85]

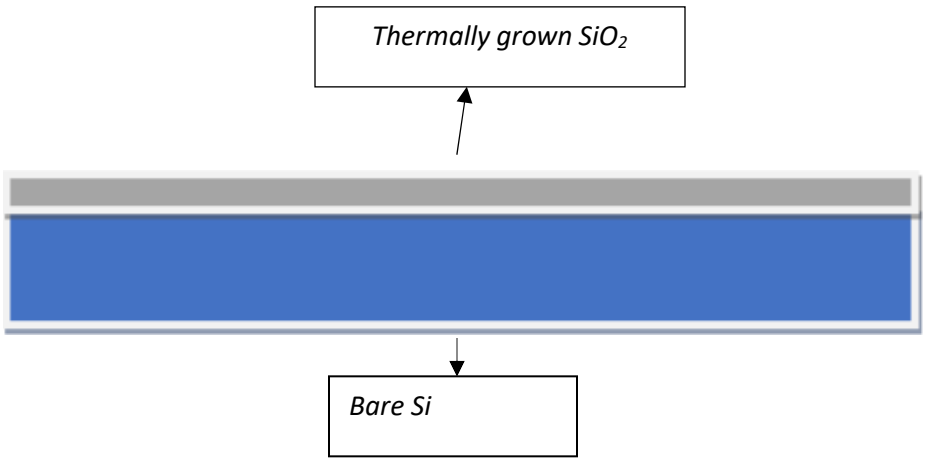

Fig:6 P-Si wafer with thermally grown SiO_2

2.7 Wet Etching

In wet etching, chemical reactions are used to remove the material selectively. To protect the area from the etchant, we use the lithography technique where resist or hard masks are placed on the area to be protected from the liquid etchant. Then, the rest of the area is exposed to an etchant to remove the material[88]. Wet etching can be explained in the following three steps:

1. Diffusion of liquid etching solution into the structure, which must be removed.
2. The reaction between the liquid etchant and the etched material. Usually, these reactions are redox reactions, as this reaction involves the oxidation of the material and the dissolution of the oxidized material.

3. Diffusion of reaction by-products from the reaction surface. [89]

In Silicon dioxide, wet etching aqueous hydrogen Fluoride-based solution can be used. In an aqueous solution, the surface of SiO2 forms the SiOH group. The substitution of a surface SiOH group, which is bonded to three bridging oxygen atoms, by a SiF group. Due to the silanol groups' acid/base equilibrium reaction on the surface with its protonated and deprotonated form. As the SiF4 is a volatile by-product with a boiling point of 4C, it is evaporated, and it exposes a new SiO2 surface, and the reaction is continued. [90]

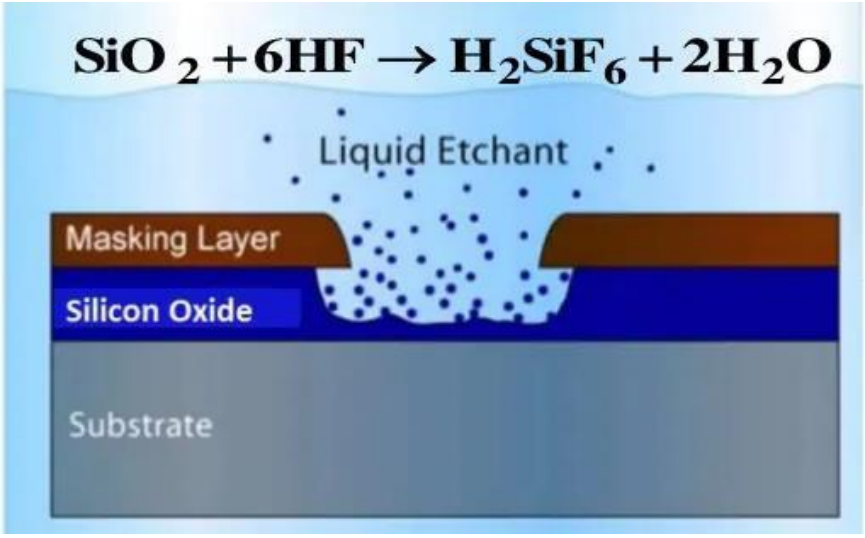

Fig:7Schematic for wet etching[91]

2.8 Scanning Electron microscopy

With significant light, humans can identify elements that are 2mm apart. With the help of a light microscope, we can achieve a magnification of about 1000x. However, the microscope's resolving power was limited by the number and quality of the lenses and incident light used for illumination.

In a scanning electron microscope (SEM), a focused electron beam is bombaded over a substrate to create an image. The incident electron beam interacts with the substarteand genrates genrating signals which are studied to understand the topgraphy structure and composition of the sample

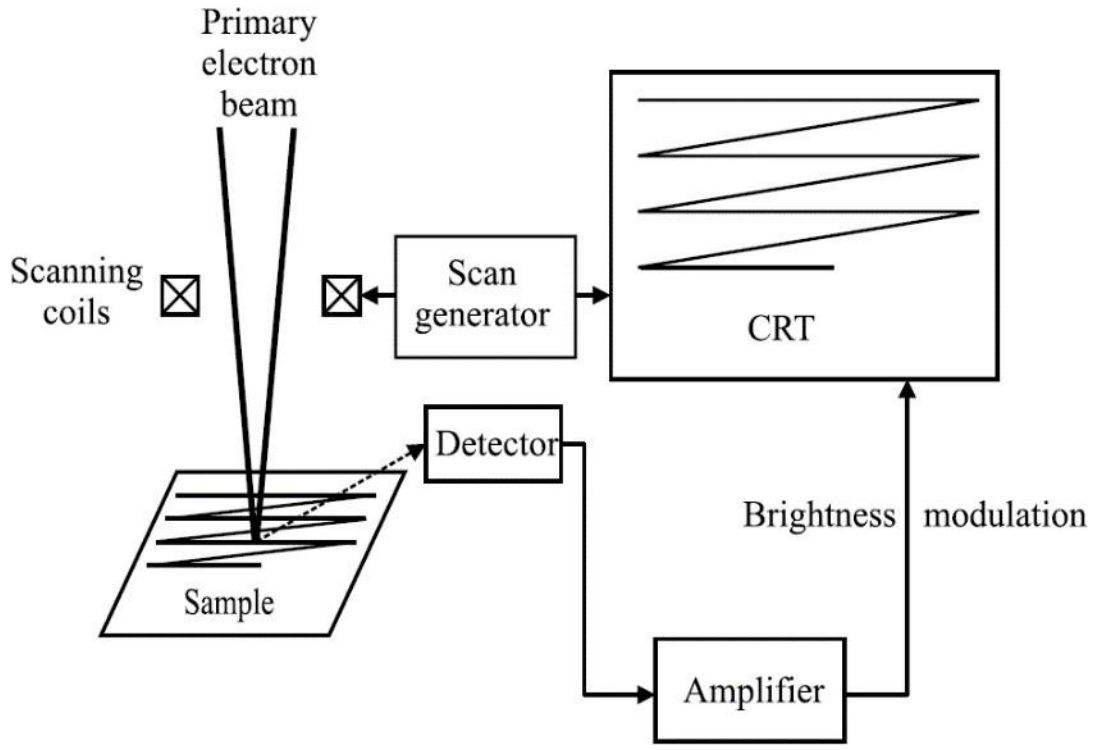

Fig.8 working of Scanning electron microscopy (SEM)[92]

In the process of scanning focused electron beam scans the surface of the specimen with the help of a cathode ray tube (CRT) to move the electron beam. These electrons are accelerated at high speed using a bias of 20KV; as they hit the specimen, they emit secondary electrons. The Electron detector is designed to collect secondary electrons that strike on the scintillator. It produces light passed through the photomultiplier, and the electronic signal from the photomultiplier is proportional to the received secondary electrons. This information can be

projected on the screen as the CRT scan the substrate line by line.[93] In a Secondary electron detector, there are two types

(a) SE Mode: - In this mode, the inelastic scattering from the incident beam is used. It is mainly used to understand the topography of the sample.

(b) BSE Mode: - In this mode, the elastic scattering from the incident beam is used. It is mainly used for showing the different elements present in the sample as the elastic scattering happens when the incoming electron interacts with the nucleus. So as the nucleus size increases, the number of BSE electrons increases[94].

(c) EDX Mode: - The way EDX analysis works is that an electron beam hits an atom's inner shell, knocking an electron out and leaving a positively charged electron-hole. When an electron is displaced, another electron from an outer shell is drawn to replace the void. This energy difference can be discharged in the form of an X-ray as the electron passes from the outer higher-energy to the inner lower-energy shell of the atom. These X-energy rays are particular to the element and transition in the sample.

2.9 UV-Vis Spectroscopy

Ultraviolet-visible (UV-Vis) absorption spectroscopy measures the absorption of the transmitted electromagnetic spectrum depending on the sample after reflection from the sample. Where the ultra-violate region is subdivided into ultra ulta-violate region (10nm - 200nm) & ultraviolet region (200nm – 400nm) while the visible region extends from 400nm to 800nm. which follows the principle of the Beer lambert law it according to which the absorption of the light by a material is directly proportional to the path length and concentration of the same[95, 96]

$A=log_{10}(I_0/I) = \varepsilon cl$

Where, A=absorbance, I_0=intensity of light incident upon sample cell, I=intensity of light leaving sample cell, c=molar concentration of solute, l=length of the sample cell. ε=molar absorptivity.

So, when light falls on the sample, each material absorbs a specific range of the electromagnetic spectrum. After absorbing, the radiation electron from the atom excites towards the higher state (Lowest unoccupied molecular orbit) from, the lower energy state (Highest occupied molecular orbit). Since various energy Levels of molecules are quantized, a particular electronic excitation occurs only by the absorption of a specific wavelength of the radiation corresponding to the required

quantum of energy[97].

From the absorbed radiation information, we can detect the Chromophore functional group[98], Identify compound/material[99], Impurities present in the sample[98]

Chapter 3 Experimental procedure

3.1 Experimental process Overview

To Form a fully saturated satellite structure by hybridizing DNA, we prepare a P-Si wafer. To get a clean surface for future processes, we clean the wafer with piranha solution, a mixture of H_2SO_4 and H_2O_2 in the ratio of 3:1. Piranha solution removes any organic compound present on the surface, followed by a thorough cleaning in Deionized water. After treating the wafer with piranha solution, we etch off any native oxide that may be present on the wafer using Hydrofluoric acid. Initial cleaning of the wafer, we load it into the Tyster oven to thermally grow approximately 100 nm of sacrificial SiO_2. After which, we cut the wafer into individual samples, then get rid of the sacrificial oxide and store it in ethanol.

These samples are individually processed first to grow SAM's layer of APTES followed by placement of C-50then Passivation of the SAM's layer followed by hybridization of target and P30.

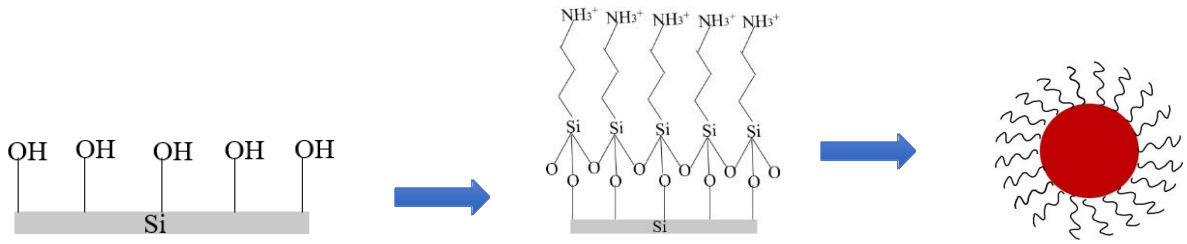

Clean individual sample *Growth of APTES SAM's Application of C50*

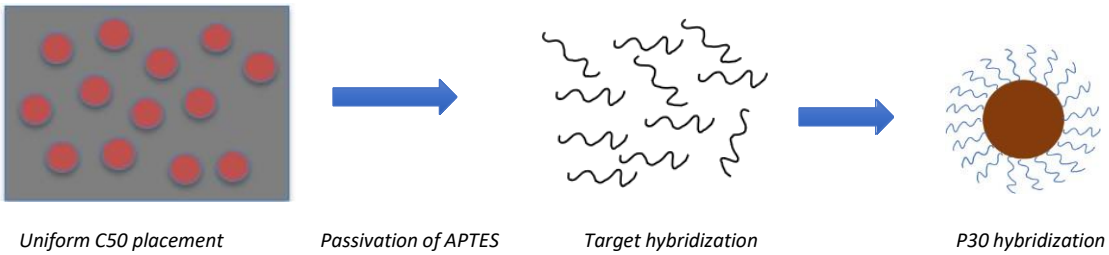

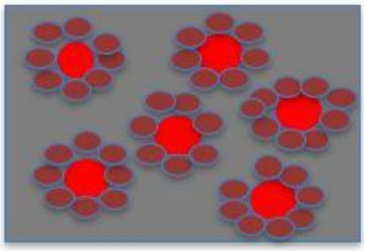

Fully saturated nanostructures

Fig.9 Schematic representation of the experimental procedure

3.2 Tools and equipment's used

- Tystar, Oxidation Furnace
- Ocean optics reflectometer
- Gaertner stokes ellipsometer
- Branson 2501, Ultra-Sonication Bath
- Disco DAD3220 Automatic Dicing Saw
- Cole-Parmer HP30A Photolithography Hot Plate
- ZEISS Supra 55 VP Scanning Electron Microscope
- Millipore DI water purification system
- Weighing Scale

- Eppendorf 5418, Centrifuge
- Vortexes

3.3 Reagents, Chemicals, and Materials used

- P-Type (100) Si wafer, Nova Electronic Materials
- Sulfuric acid solution
- Hydrogen peroxide solution
- DI water
- Liquid Acetone
- Liquid ethanol
- Liquid methanol
- Liquid IPA
- Hydrogen fluoride solution
- Synthetic oligonucleotide probe-DNA with disulfide linker, BioBasi
- Synthetic oligonucleotide probe-DNA with disulfide linker, BioBasi
- Synthetic oligonucleotide probe-DNA with disulfide linker, BioBasi
- Synthetic oligonucleotide probe-DNA with disulfide linker, BioBasi
- DL-Dithiothreitol (DTT), Sigma-Aldrich
- 30nm Gold Nanospheres, Bare (Citrate), NanoComposix
- 50nm Gold Nanospheres, Bare (Citrate), NanoComposix
- NAP-5 filter column, GE Healthcare
- Sodium Chloride (>99.5%), Sigma-Aldrich

- Sodium Hydroxide, Sigma-Aldrich
- Tris-EDTA buffer solution, Sigma-Aldrich
- 3-Aminopropyltriethoxysilane (APTES), Sigma-Aldrich
- Sodium phosphate monobasic monohydrate, Sigma-Aldrich
- Sodium phosphate dibasic heptahydrate, Sigma-Aldrich
- Hydrochloric acid-bio grade, Sigma-Aldrich
- Saline–Sodium Phosphate–EDTA, Sigma-Aldrich
- Triton solution Sigma-Aldrich, Sigma-Aldrich
- Dimethyl sulfoxide-DMSO, Sigma-Aldrich
- Denhardt solution Sigma-Aldrich, Sigma-Aldrich
- Sodium dodecyl sulfate Sigma-Aldrich, Sigma-Aldrich
- AC-MMP, Biomag Plus

3.3 DNA-Gold nanoparticle conjugation

To create fully saturated nanoparticle satellite structures, the first step is to functionalize the gold nanoparticles with thiolated DNA. Then, the Conjugation is done at a low Ph and adjusting the buffer strength; we have two different sequences on DNA that we conjugate on the nanoparticles, namely, Capture DNA on 50 nm AuNp termed as C50 and Probe DNA on 30 nm AuNp termed as P30.

3.3.1 Capture DNA -50Nm Gold Nanoparticle Conjugation

The Capture-DNA or C-DNA is conjugated with 50 nm AuNP to create a C-50 colloid. C-DNA has the following sequence-

In this section, we will discuss the step-by-step procedure of C50 Conjugation.

- Preparation of 0.1M DTT solution – For Cleaving the DNA

This C-DNA is a Synthetic oligonucleotide with a Disulfide linker (Disulfide linkers allow storage of DNA); this Disulfide bond must be broken before adding DNA to the gold nanoparticles. DL-Dithiothreitol (DTT) is used to do so. We used 0.1M of DTT in Phosphate buffer (PB)-0.2M pH-8. To achieve 0.1M DTT, 0.0154g of DTT powder is required for 1 ml of phosphate buffer to prepare 0.1M DTT. To do so, we Take out the DTT bottle from the refrigerator and leave the bottle at RT for 30 min (to prevent the moisture built-up). Once the DTT is at room temperature, we Prepare a test tube and weigh DTT on a scale by putting the DTT power into the test tube then Pipette the correct volume of PB (0.2M PB, pH 8) into the test tube and shake the test tube in a vortex shaker till all the powder is dissolved in the buffer. Once all the powder is dissolved and we get a clear solution, the 0.1M DTT solution is ready

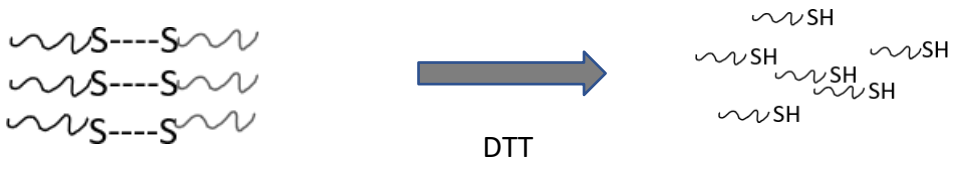

Fig10. Schematic for working of DTT

- Cleavage of Disulfide bonds

With the above made 0.1M DTT solution, we can cleavage the Disulfide linkers.

- we first take out the DNA tube from the freezer
- Set the DNA at room temperature for 30 minutes.
- Centrifuge the DNA tube at 3,000 rpm for 3 minutes (this lets the DNA settle at the bottom of the tube).
- Pipette 120 micro-liters of the 0.1M DTT solution into the DNA tube. (We must be Careful that we release the DTT solution at the bottom of the tube).
- Wait for 2 minutes; this allows the DNA to rehydrate. Then Mix the tube by hand for a minute mix the DNA and DTT.
- Wrap the tube with an Aluminum foil and vortex (at the lowest speed) for 2 ½ hours.

Once the Disulfide bond is cleaved, the DNA needs to purify, i.e., it needs to be separated from the DTT. We used NAP-5 columns to purify DNA from the DTT solution.to do so, we use Nap-5 columns

- DNA Purification using Nap-5

The NAP -5 columns filter the oligonucleotides in the DNA-DTT solution by their size. As these columns are made up of porous matrix structure which can filter and allow small size oligonucleotides only and blocks all large size molecule

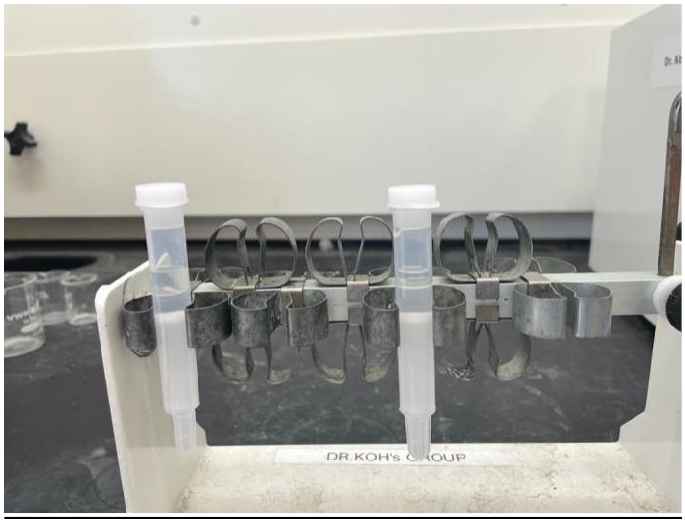

Fig.11 Nap5 Columns

We follow the steps given below for Purifying the DNA in DTT using NAP-5 columns

- Take the NAP-5 filter column out from the fridge.
- Allow it to equilibrate under room temperature for at least 1 hour
- Remove both top and bottom caps and let the storage buffer drain completely.
- Pipette 15mL of fresh DI water into the filter column (1mL each time, total 15 times).
- Let it drain.
- Pipette 120µL of DNA/DTT into the filter column.
- Let it drain.
- Pipette 480µL of DI water into the filter column.
- Let it drain
- Pipette the last 300µL of DI water into the filter column.
- Collect the 300µL DNA/DI drain droplet in a new test tube

The Final collected 300 µL solution is the purified DNA in DI solution

- Preparation of Nanoparticles

Once we prepare the Pure DNA in DI solution,the next step is to prepare the nanoparticles for Conjugation.

- Collect 2mL of 30nm gold nanoparticle colloid in the test tube.
- Centrifuge the gold nanoparticle colloid at 4000 rcf for 10 minutes.
- Take out 1950µL of the gold nanoparticle colloid supernatant.
- Shake well the rest of 50µL gold nanoparticle.

- Procedure to be followed for Capture DNA-AuNp conjugation (Half-Citrate Approach)

The conjugation procedure is done at 65^0C. To do so, we heat the above-purified DNA in DI solution and 50 nm AuNp at 65^0C for 5 minutes in a dry bath. While doing so, we mix 84 µL of 500mM citrate buffer and 25.4 microliters of HCl and heat the mixture at 65^0C. Once all the above solutions reach 65^0C. we follow the following steps for conjugations

- With quick mixing, pipette 10.94 µL of Citrate buffer and HCl solution in DNA/Di solution.
- Incubate the solution for 30 seconds.
- Mix the entire DNA/DI solution to pre-heated Nanoparticles by mixing with parts 15 µL*2 times then. Then 30 µL*4time then 75 µL*2 times.
- Incubate the nanoparticles for 150 seconds in a heater at 65^0C-this allows a dense DNA attachment to nanoparticles.

- After the incubation, add 8.4 µL of 500 mM Citrate Buffer; this makes the concentration of citrate buffer 20 µM.
- Incubate 150 seconds in the heater at 65^0C.
- While incubating the nanoparticles, we shake the solution once in a while.
- Add 18.6 µL of 1M NaOH; this will increase the pH of the solution to approximately 6.0.
- Pipette 580µL of Tris-EDTA buffer into the conjugates, handshake well.
- Transfer the conjugates into a new test tube
- Centrifuge at 3000 rcf for 10 minutes.
- Take out the supernatant and resuspend in 950 µL Tris-EDTA buffer (pH8) 48.
- Repeat above three purification steps three more times
- Finally, add 800 µL of TE buffer
- Adjust the concentration of the colloid to 2 OD and store the conjugates in the fridge

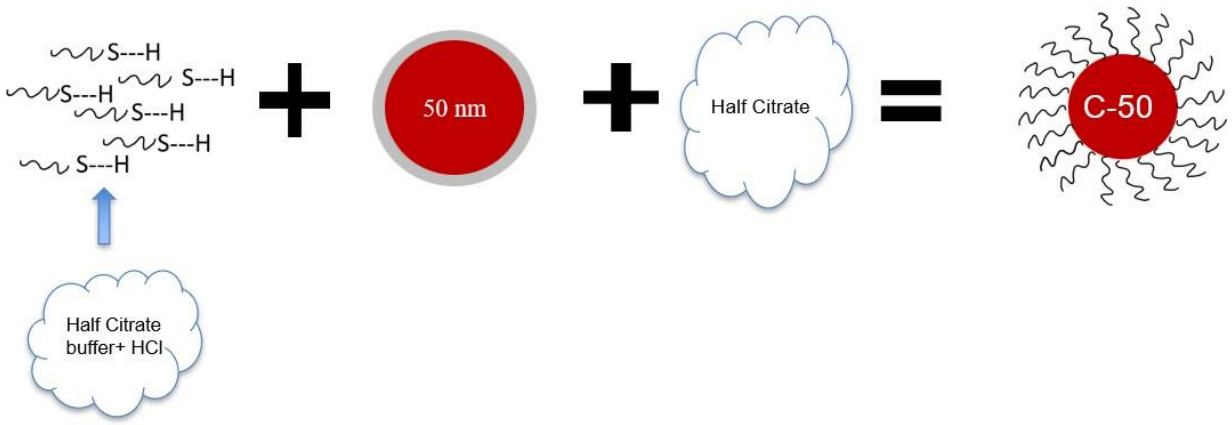

Fig.12 Schematic for C50 Conjugation

- Adjustment of colloid concentration

The colloid concentration stored in the refrigerator needs to be adjusted to 2 OD.

So, the exact concentration of C50 can be controlled during Satellite structure formation. To do so, we use the Nanodrop UV-Vis

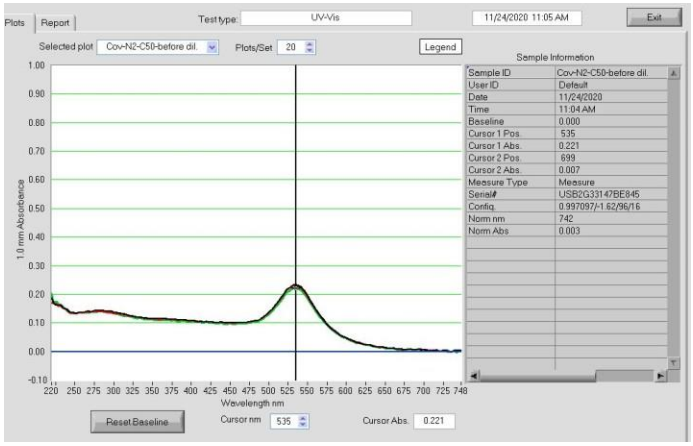

Fig 13 UV-Vis Plot Before adjusting concentration -C-50

- Adjust the concentration of the colloid to exact 2X using the Beer-Lambert Law

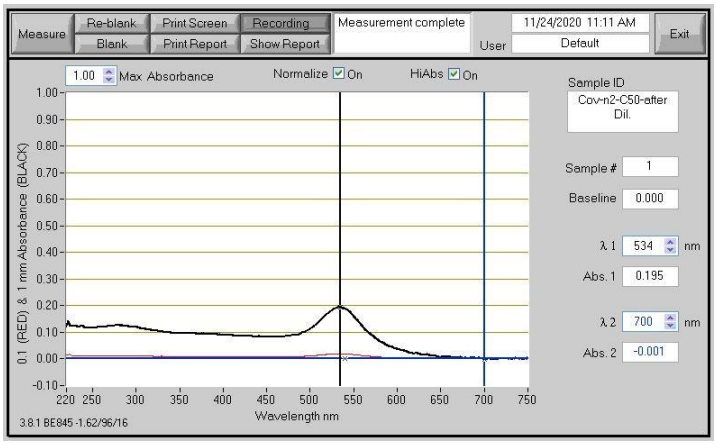

Fig 14 UV-Vis Plot after adjusting concentration -C-50

- These Capture DNA functionalize AuNP are stable even in 2M NaCl

3.3.2 Probe DNA Conjugation

The Probe-DNA or P-DNA is conjugated with 30 nm AuNP to create a P-30 colloid. P-DNA has the following sequence:

- **Preparation of 0.1M DTT solution**

This C-DNA is a Synthetic oligonucleotide with a Disulfide linker (Disulfide linkers allow storage of DNA); this Disulfide bond must be broken before adding DNA to the gold nanoparticles. DL-Dithiothreitol (DTT) is used to do so. We used 0.1M of DTT in Phosphate buffer (PB)-0.2M pH-8. To achieve 0.1M DTT, 0.0154g of DTT powder is required for 1 ml of phosphate buffer to prepare 0.1M DTT. To do so, we Take out the DTT bottle from the refrigerator and leave the bottle at RT for 30 min (to prevent the moisture built-up); once the DTT is at room temperature, we Prepare a test tube and weigh DTT on a scale by putting the DTT power into the test tube then Pipette the correct volume of PB (0.2M PB, pH 8) into the test tube and shake the test tube in a vortex shaker till all the powder is dissolved in the buffer. Once all the powder is dissolved and we get a clear solution, the 0.1M DTT solution is ready

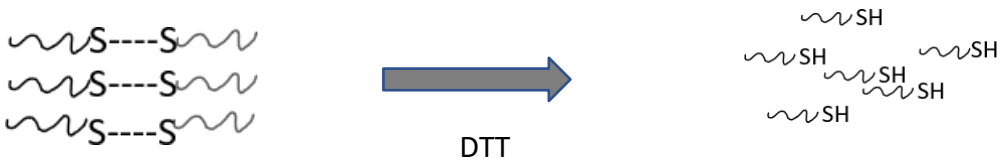

Fig.15 Schematic for working of DTT

- **Cleavage of Disulfide bonds**

With the above made 0.1M DTT solution, we can cleavage the Disulfide linkers to do so

- we first take out the DNA tube from the freezer
- Set the DNA at room temperature for 30 minutes.
- Centrifuge the DNA tube at 3,000 rpm for 3 minutes (this lets the DNA settle at the bottom of the tube).
- Pipette 120 micro-liters of the 0.1M DTT solution into the DNA tube. (We must be Careful that we release the DTT solution at the bottom of the tube).
- Wait for 2 minutes; this allows the DNA to rehydrate. Then Mix the tube by hand for a minute mix the DNA and DTT.
- Wrap the tube with an Aluminum foil and vortex (at the lowest speed) for 2 ½ hours.

Once the Disulfide bond is cleaved, the DNA needs to purify, i.e., it needs to be separated from the DTT. We used NAP-5 columns to purify DNA from the DTT solution.to do so, we use Nap-5 columns

- **DNA Purification using Nap-5**

The NAP -5 columns filter the size of the oligonucleotides in the DNA-DTT solution. As these columns are made up of porous matrix structure which can filter and allow small size oligonucleotides only and blocks all large size molecule

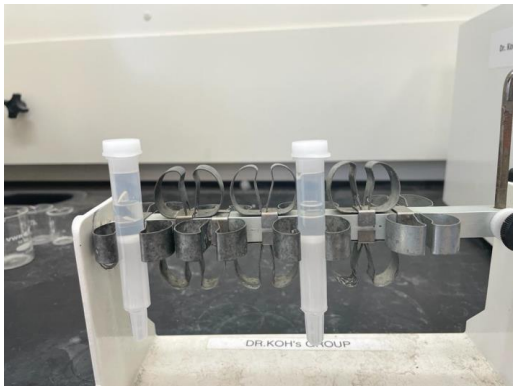

Fig16.Nap5 column's

We follow the steps given below for Purifying the DNA in DTT using NAP-5 columns

- Take the NAP-5 filter column out from the fridge.
- Allow it to equilibrate under room temperature for at least 1 hour
    - Remove both top and bottom caps and let the storage buffer drain completely.
    - Pipette 15mL of fresh DI water into the filter column (1mL each time, total 15 times).
    - Let it drain.
    - Pipette 120µL of DNA/DTT into the filter column.
    - Let it drain.
    - Pipette 480µL of DI water into the filter column.
    - Let it drain
    - Pipette the last 300µL of DI water into the filter column.
    - Collect the 300µL DNA/DI drain droplet in a new test tube

The Final collected 300 µL solution is the purified DNA in DI solution

- Preparation of Nanoparticles

Once we prepare the Pure DNA in DI solution, we then prepare the nanoparticles for Conjugation

- We use Citrate capped 30 nm AuNP from Sigma Aldrich
- Collect 2mL of 30nm gold nanoparticle colloid in the test tube.
- Centrifuge the gold nanoparticle colloid at 4000 rcf for 10 minutes.
- Take out 1950µL of the gold nanoparticle colloid supernatant.
- Shake well the rest of 100µL gold nanoparticle.

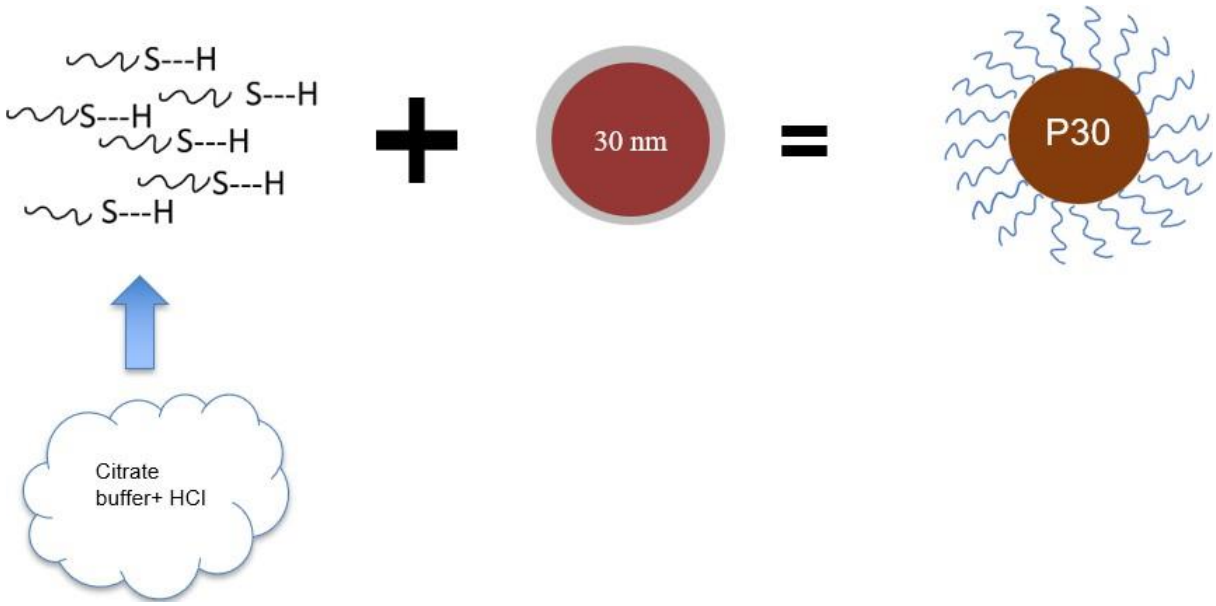

Fig.17 Schematic for P30 Conjugation

- **<u>Procedure to be followed for Capture DNA-AuNp conjugation (Half-Citrate Approach)</u>**

The conjugation procedure is done at 65^0C. To do so, we heat the above-purified DNA in DI solution and 30 nm AuNp at 65^0C for 5 minutes in a dry bath. While doing so, we mix 167.7µL of 500mM citrate buffer and 25.4 microliters of HCl and heat the mixture at 65^0C. Once all the above solutions reach 65^0C. Then, we follow the following steps for conjugations.

- With quick mixing, pipette 19.31 µL of Citrate buffer and HCl solution in DNA/Di solution.
- Incubate the solution for 30 seconds.
- Mix the entire DNA/DI solution to pre-heated Nanoparticles by mixing with parts. As 15 µL*2 times then. Then 30 µL*4time then 75 µL*2 times.
- Incubate the nanoparticles for 300 seconds in a heater at 65^0C-this allows a dense DNA attachment to nanoparticles.
- While incubating the nanoparticles, we shake the solution once in a while.
- Pipette 580µL of Tris-EDTA buffer into the conjugates, handshake well.
- Transfer the conjugates into a new test tube
- Centrifuge at 3000 rcf for 10 minutes.
- Take out the supernatant and resuspend in 950 µL Tris-EDTA buffer (pH8) 48.
- Repeat above three purification steps three more times
- Finally, add 800 µL of TE buffer
- Adjust the concentration of the colloid to 2 OD and store the conjugates in the fridge

- **<u>Adjustment of colloid concentration</u>**

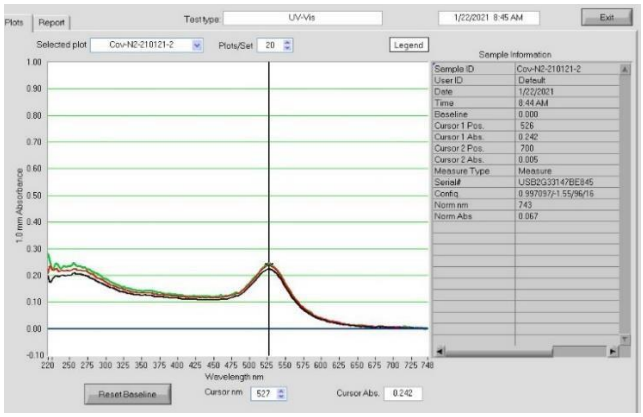

Fig 18. UV-Vis Plot before adjusting the concentration of P30

- Adjust the concentration of the colloid to exact 2X using the Beer-Lambert Law

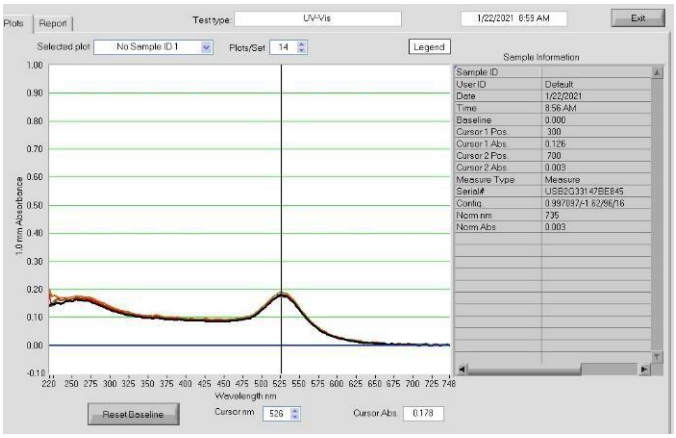

Fig 19. UV-Vis Plot after adjusting the concentration of P30

These Probe DNA functionalize AuNP are stable in 2M NaCl

3.4 Sample Preparation.

- **wafer Cleaning**

We use a 4-inch Psi wafer. The first step in sample preparation is to clean the samples in piranha solution, followed by 10:1 Hydrofluoric acid cleaning. The piranha solution is a 3:1 mix of Sulfuric acid and Hydrogen peroxide. The piranha solution is prepared in an open Glass beaker; Proper safety must be taken while handling. This removes any organic waste on the wafer.

We must be sure that the piranha is freshly prepared every time. As soon as piranha solution is made, follow the following procedures:

- Immerse the wafer into the piranha solution for 30 minutes.
- Transfer wafer to a DI water container for 5 minutes *2.
- Wash it under running DI water.
- Dry with N2.

After cleaning the wafer in piranha solution, we clean the wafer in 10:1 Hydrofluoric acid. This step gets rid of any native oxide grown on the wafer

The HF cleaning is done as follows

- Immerse the wafer into the Hydrofluoric acid for 10 minutes
- Transfer wafer to a DI water container for five minutes two times and dry with N_2

- **Thermal Oxidation**

In this step, a sacrificial layer of 100 nm of SiO_2 Is Grown on the P-Si wafer. This layer is grown to prevent any contamination of the Si wafer surface due to the cooling liquid used during the Dicing of the wafer.

Step	Time	Temperature	Gas flow
Idle temp	NA	450C	NA
Boat out/in	15 mins	450C	NA
Ram up	30 mins	700C	5000 SCCM N2
Stabilize	30 mins	700C	5000 SCCM N2
Ramp-up	1 hr.	1000C	5000 SCCM N2
Hold	2Hr 40 mins	1000C	3000 SCCM O2
Anneal	20 mins	1000C	5000 SCCM N2
Ramp Down and hold	2 hrs. and wait till the alarm acknowledges	700C	5000 SCCM N2

Table 1-thermal Oxidation conditions in the furnace

Fig20.Thermally grownSiO2

- **<u>Individual Sample Preparations</u>**

This recipe typically grows~100nm to 145 nm of SiO_2. After thermally growing SiO_2, we dice the wafer in 6mm by 9mm samples using a dicing tool.

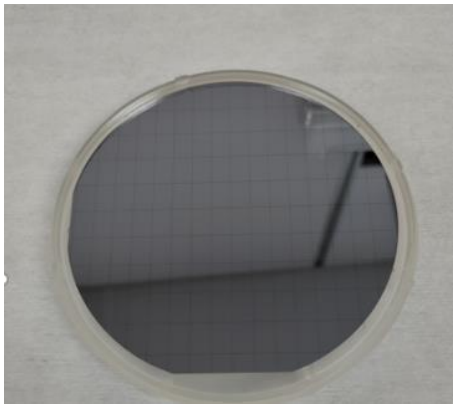

Fig 21. Diced wafer

Fig.22 Cleaned individual sample

After Dicing the Wafer, we etch the sacrificial oxide using 10:1 HF and then clean the samples using the following steps

- Acetone Sonication (10 minutes).
- Cleaning with IPA using Squeeze bottle IPA.

- IPA Sonication (10 minutes).
- UV-zone cleaning for 30 minutes. (to grow hydroxyl terminations)
- Acetone Sonication (10 minutes).
- IPA Sonication (10 minutes).
- Cutting the diced wafer into individual samples.
- IPA Sonication (10 minutes).
- Store these cleaned samples with hydroxyl termination on the surface in ethanol

3.5 Formation of Satellite Structures

The formation of satellite structures is a multi-step process. The first step is to grow the SAMS layer of APTES to make the Si surface positively charged. In the next step, we uniformly place the C-AuNp. Further, we passivate the Positively charged Si substrate with Sulfo-SMCC, we hybridize the C-DNA AuNP with the target first and P-DNA AuNP later. The detailed and step-by-step process is described below.

- **APTES SAM's Layer formation**

The first step is to guide the DNA functionalized nanoparticles and place them uniformly on the Si substrate to charge the Substrate positively. The Positive charge on the Si substrate is achieved by growing a SAM's layer of APTES on the Substrate. We used the samples that were stored in ethanol.

Prepare a test tube (2mL)

• Pipette 950µL of pure ethanol into the tube

- Pipette 30µL of pH 13 DI water into the tube
- Pipette 20µL of APTES into the tube
- Vortex the total 1000µL of APTES mixture solution for 10 seconds (highest speed)
- Rinse the sample with the ethanol squeeze bottle
- Immerse it in the APTEX mixture solution for 60 minutes
- Prepare wash step tubes (6 of them)
- Pipette 1mL of pH 13 ethanol for each first three tubes
- Pipette 1mL of pure ethanol for each remaining three tubes
- Rinse the sample in each tube for 30 seconds
- N2 dry
- Bake the sample on a Hot plate at 120^{o}C for 10 minutes; this allows crosslinking of the monolayers

Ensure to wash the tweezer by ethanol squeeze bottle every time the substrate transfers to the next tube; also, between the third and fourth tube, rinse the sample with the ethanol squeeze bottle because the ethanol pH has a significant change from pH 13 to pH 7.

- **<u>Preparation of Capture DNA</u>**

- Take 25 µL C50 colloid with concentration 2 OD in a test tube and add 275 µL 0.1 mM Phosphate buffer with pH~7.
- Centrifuge at 3000 rcf 10 min, take out the supernatant and resuspend in 300 µL 0.1 mM Phosphate buffer pH 6.84
- Centrifuge at 3000 rcf 10 min, take out the supernatant and resuspend in 20 µL 0.1mM Phosphate buffer.
- The final colloid is C-DNA AuNp with 2.5 OD and is ready for placement on the APTES grown Si wafer

- **Application of Capture DNA**

- Apply five µL of Cov-N2-C50 on the prepared Substrate with the APTES SAMS layer for 10 minutes.
- Prepare 4test tubes with DI water for washing the Substrate
- After 10 minutes of C50 placement, rinse the Substrate with DI in tube 30 sec twice, followed by a quick rinse by squeeze bottle DI and then again Rinse with DI for 30 sec per tube

Immediately after rinsing the Substrate in DI, we passivate the positive charge on the Si substrate using Sulfo-SMCC.by doing so, and we ensure a systematic hybridization between Capture DNA, the target DNA, and probe DNA in the following steps.

- **Passivation of APTES Layer**

- To passivate the positive charge on the Si surface due to APTES, we use Sulfo-SMCC.

- To prepare 5nM Sulfo-SMCC, we weigh0.0022g of the Sulfo-SMCC powder and mix it with1.08ml 1XPBS Buffer
- Immediately after washing the sample in DI, we Immerse into five mM Sulfo-SMCC in 1X PBS (pH 7.4) for 30 min
- After immersing the sample in Sulfo-SMCC for 30 minutes, we wash the sample with DI in tube 30 sec (X2): squeeze bottle DI; Rinse with DI in tube 30 sec (X2)

After rinsing the sample in DI, we dip the sample in ethanol and then dry the sample with N2 gas.

- **Target and Probe DNA -AuNP placement**
- **Preparing Hybridization buffer**

To facilitate the Hybridization of target and Probe DNA, we prepare Them in a Hybridization buffer solution. This solution is made by mixing 0.1% Triton solution and 10% Dimethyl sulfoxide solution (DMSO) with DI and Saline–Sodium Phosphate–EDTA(SSPE). The volume of SSPE and DI is changed by the desired concentration. The table below shows volumes of solutions needed to make the desired concentration of hybridization buffer.

SSPE Concentration	Target volume mL	The volume of Denhardt used µL	The volume of SSPE used µL	The volume of DMSO used µL	Volume of triton used µL	The volume of DI used µL
8XSSPE	40	1600	16000	2000	40	18370
6XSSPE	40	1600	12000	2000	40	22370
4XSSPE	40	1600	8000	2000	40	24370
3XSSPE	40	1600	6000	2000	40	28370
2XSSPE	40	1600	4000	2000	40	30370
1XSSPE	40	1600	2000	2000	40	32370

Table.2 Hybridization buffer calculation

- **Preparing target**

To prepare the Target DNA solution, we need the following materials

Materials

- Vial of COV-N2-T
- The target sequence is listed below

(TTACAAACATTGGCCGCAAATTGCACAATTTGCCCCCAGCGCTTCAGCGTTCTTCGGAATGTCGCGC)

- Hybridization buffer
- TRIS-EDTA buffer

Procedure

- Centrifuge the vial of the target at 3000 rpm for three minutes-this allows the DNA to settle down at the bottom of the tube
- Add 1.55 mL of Tris EDTA(T.E.)) buffer and shake well in the rotational shaker at least for 20 minutes
- Transfer half of it (775 mL) to a new tube creating two tubes of the target, each with a total of 775 µL target DNA in TE buffer
- Add 775 mL TE to each of the two tubes. This makes the total volume of target two tubes to 3.1 mL and concentration of target as one mM (3.3 nmol/3.3mL)
- Make aliquots where each aliquot will have a total off 20 µL target
- Store them in the freezer
- Take out one aliquot 20 µL from the freezer
- Pipette 10 µL of 1uM target and add 90 µL 4Hybridization Buffer (concentration of the buffer can change as per requirement) This makes the concentration of target to 100nM
- Pipette 10 µL of 100nM target and add 190 µL Hybridization Buffer to it this makes the concentration of target to 5nM

- **Preparing Probe DNA**

- Pipette 25 mL P30 (2X) into a tube
- Centrifuge at 3000rcf 10 min, take out the supernatant and resuspend in 200µL HB.
- Centrifuge at 3000rcf 10 min, take out the supernatant and resuspend in 200 µL HB.
- Centrifuge at 3000rcf 10 min, take out the supernatant and add ten µL of HB.

- This makes the final concentration of the nanoparticles to be 5X.
- After Passivating the APTES SAM's layer, we follow the following procedure to form a satellite structure
- **Target Hybridization**
  - Pipette 5 µL 5 nm. target in HB, 10 min at room temperature
  - After 10 minutes for hybridization, we perform a set of stringency washing as Immerse into pre-HB (without Denhardt solution) buffers for 15sec and repeat the same twice
  - Then immerse the sample in Hybridization Buffer
  - Then put the wafer in a drip tube to allow the sample to dry enough to form a thin film on the Substrate
  - Once a thin film of Hybridization buffer is formed on top of the Substrate, apply 10 mL of the Previously prepared Probe DNA (5X) concentration in the hybridization buffer for 10 minutes
  - Repeat the stringency washing steps followed by target placement
  - After the stringency washing is done, we put the wafer in a drip tube so that the sample naturally dries
  - Once the sample is completely dried, we clean the sample with repetitive dipping the sample in DI then ethanol and drying with N2 for 5 seconds each dip

Chapter4. Result and discussions

To make the process robust and reproducible, hybridization parameters like temperatures and buffer strength are varied. This chapter discusses the changes done in these parameters and the outcome of those variations. Further, this chapter also focuses on the problems seen on the Si substrate, which could hinder the formation of satellite structure, and describes the solutions to overcome those issues.

4.1 Hybridization Buffer

The first parameter tested to make the procedure robust was varying the hybridization buffer strength. Increasing the hybridization buffer strength means increasing the salt concentration in the buffer. It is seen from the literature that increasing salt concentration facilitates the hybridization of DNA.

We tested the following buffer strengths

Buffer strength	Approximate Salt concentration present
4XSSPE	0.596M
6XSSPE	0.894M
8XSSPE	1.192M

Table 3: Salt concentration in hybridization buffers

The target and P30 were processed in the above hybridization buffer salt strengths.

Results:

4XSSPE hybridization buffer: -

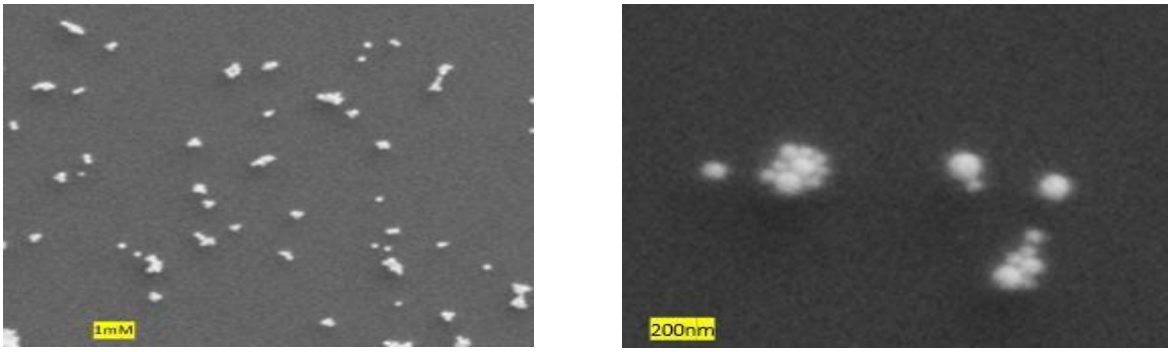

Fig.23-SEM images for hybridization done with 4XSSPE hybridization buffer

6XSSPE hybridization buffer: -

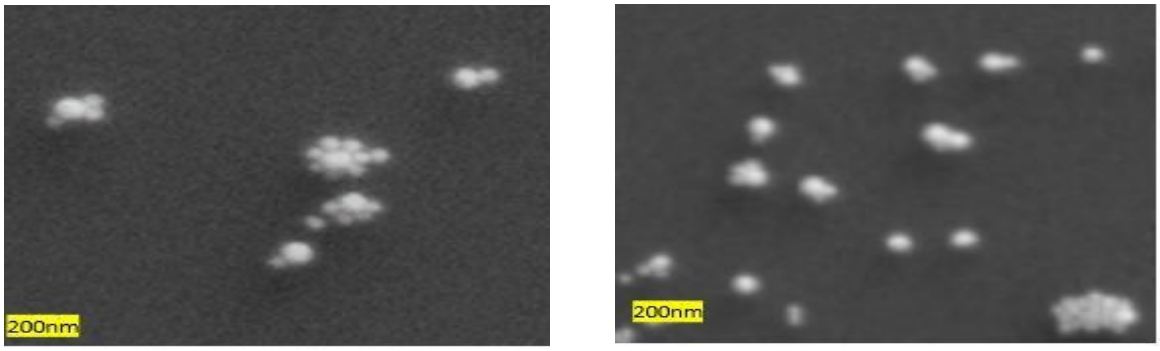

Fig.24-SEM images for hybridization done with 6XSSPE hybridization buffer

8XSSPE hybridization buffer: -

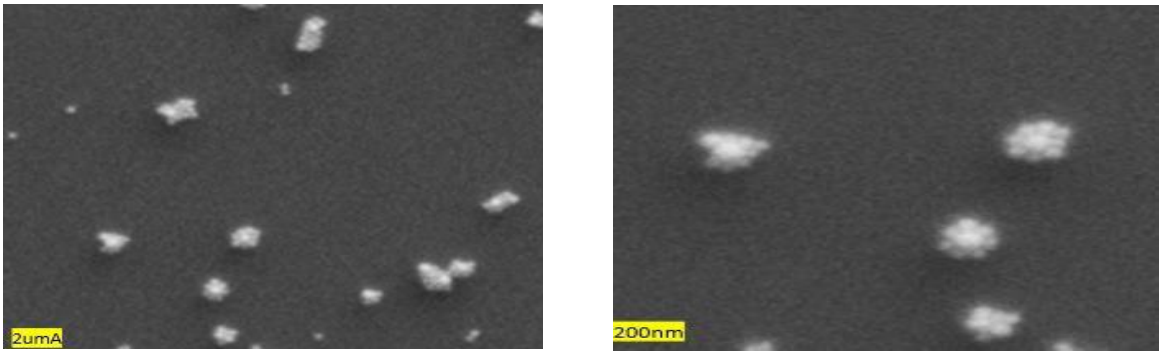

Fig.25-SEM images for hybridization done with 8XSSPE hybridization buffer

Inference

From SEM images in FIG.23, fig 24, and fig25, we see that increasing the SSPE concentration in hybridization buffer has a better attachment of P30. We were able to see some satellite structures, but the results were not consistent. There is a very high probability that by increasing the hybridization buffer strength, may have enforced nonspecific bindings of the DNA strands causing the result to be inconsistent.

Considering all these factors, we narrowed the hybridization buffer strength to 4XSSPE.

The next step was to try various hybridization temperatures and find the optimum temperature for hybridization.

4.2 Hybridization temperature

The second parameter that was tested during this project was hybridization temperature. The hybridization temperature was increased to eliminate any hairpin loop formed in the DNA,

prohibiting the target and P30 hybridization. Hybridization of target and P30 were tested at room temperature, at 50^0C, and 65^0C. The hybridization buffer strength for these samples was kept fixed at 4XSSPE to have a consistency in the data that we obtain.

Results: -

<u>Hybridization was done at room temperature:</u>

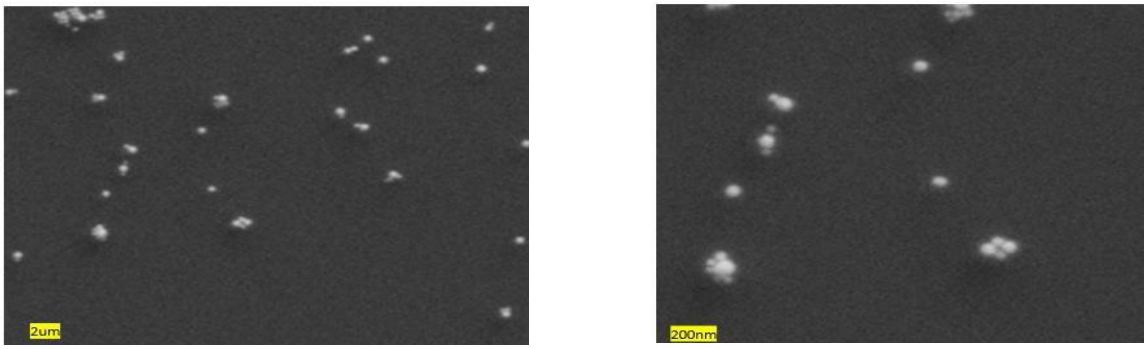

Fig.26-SEM images for hybridization done at room temperature

<u>Hybridization was done at50^0C</u>

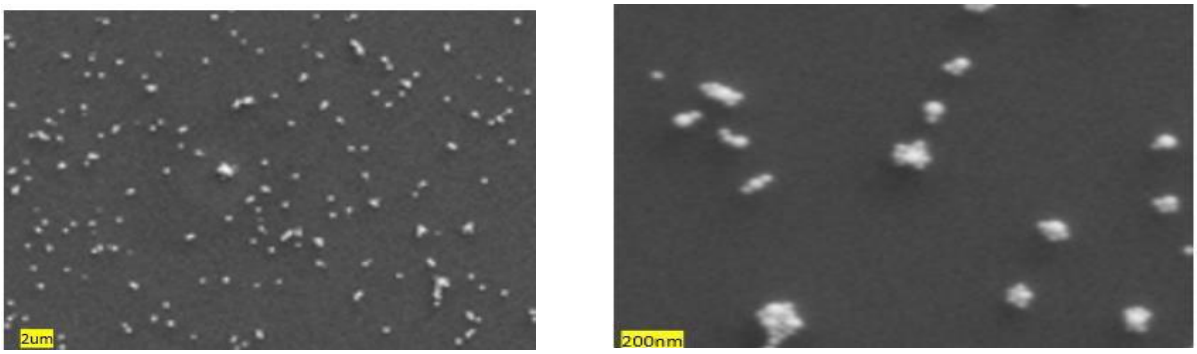

Fig.27-SEM images for hybridization done 50^0C

Hybridization was done at65^{0}C

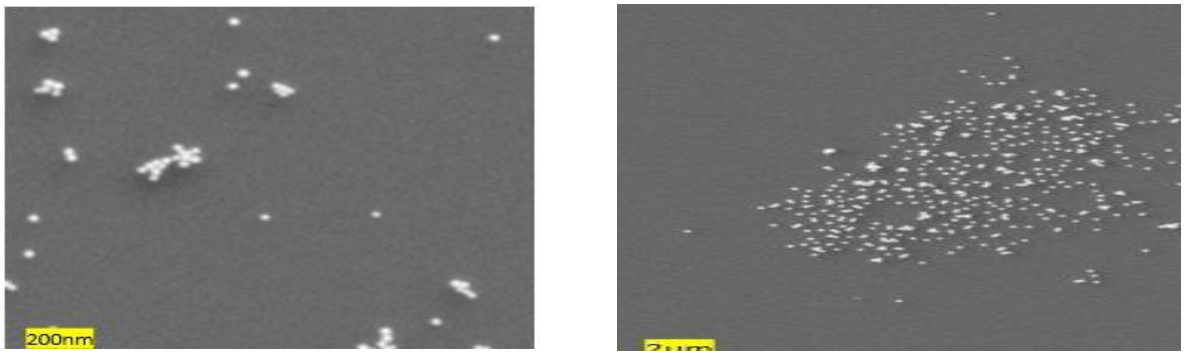

Fig.28-SEM images for hybridization done 65^{0}C

Inference

By looking at the Sem images in Fig.26 to 28, we could establish a clear difference between the structures formed at different hybridization temperatures. It was seen that a better attachment was observed when the hybridization process was carried out at 50^{0}C

Though we could get a good attachment of P30 on C50 and form some satellite structures at 50^{0}C, the process was not robust and reproducible yet.

A point to be noted here is that while the hybridization was done at higher temperatures, subsequent stringency washing was still done at room temperature. Moreover, that could create an ambiguity in the analysis of the result. And hence we tested the stringency washing at higher temperatures as well .

4.3 Use of Sodium Dodecyl sulfate SDS

As mentioned in the previous section, only doing the hybridization at higher temperatures could have created ambiguity in the outcomes of hybridization temperatures. So decided that even the Stringency washing was to be done at 50^{o}C. However, when we heated the stringency washing buffer at 50^{o}C, we found that the triton and DMSO solutions in the stringency washing buffer was turning milky. To avoid this, we replaced the Triton Solution and DMSO solution in hybridization and stringency washing buffers with Sodium Dodecyl sulfate (SDS) solution

While processing these samples, we did the hybridization at 50^{o}C, and the concentration of the hybridization buffer was 4XSSPE. After which we compared the structures formed with DSD and without SDS in hybridization and stringency washing buffers having triton and SDS

Results

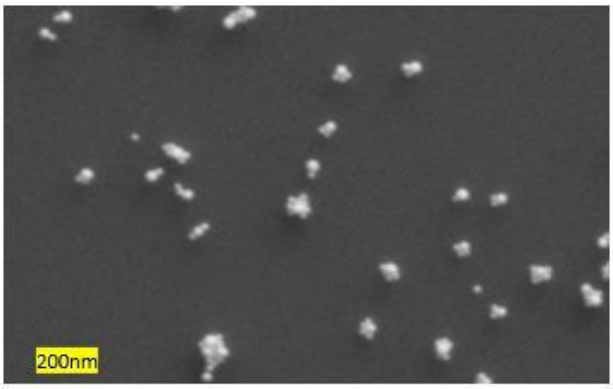

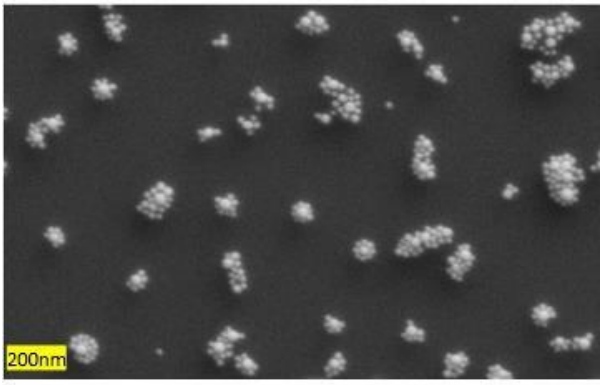

Fig. 29A *Fig .29B*

Fig29- A) Hybridization done with triton and DMSO in the buffer and 28B done with SDS in hybridization buffer

Inference

When we compared SEM images in fig. 29, a clear difference was seen between triton and DMSO solution in hybridization buffer and SDS in hybridization buffer. It was observed that using SDS in the hybridization buffer made a drastic difference in the amount of P30 attached to the C50 and the total number of satellite structures formed.

We replaced the triton and DMSO in the hybridization buffer with SDS considering the above data.

Reproducibility of structures formed using SDS

Though using SDS in the hybridization buffer gave good attachment with a lot of satellite structures, these attachments and structures were not reproducible, as seen in the SEM images in fig 30 below. Both the samples had identical experimental procedures and conditions yet differentoutcomes.

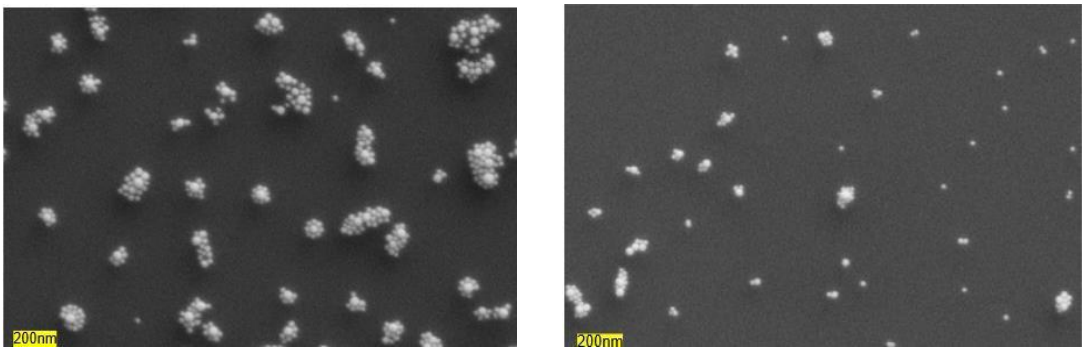

Fig. 30A *Fig .30B*

Fig 30- A) Hybridization done SDS producing good results and B) done with SDS having non-uniform attachments buffer

- **Issues Seen on the Substrate**

When we investigated the cause of inconsistency of results by analysing our SEM images we were able to seea few persistent issues mentioned below.

A. Carbon like junk on the Substrate

B. uneven and non-uniform placement of C50

C. direct attachment of P30 on the Substrate after passivation of APTES

D. Agglomeration of P30 on the Substrate

There was a high probability that these issues could have been causing inconsistency in results. Therefore, these issues were individually addressed in the following sections.

4.4 Carbon like junk on the Si substrate

While studying the SEM images in fig.31, we consistently observed patches of junk/carbon-like shoot on the bare Si substrate. This junk could create issues while forming a uniform of APTES SAMs layer.

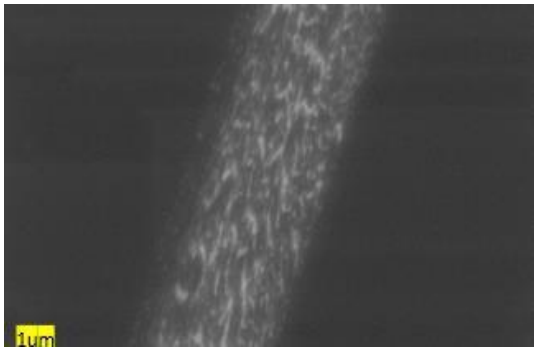

Fig.31 a

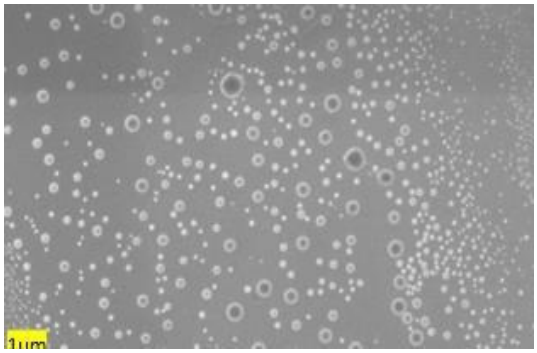

Fig.31b

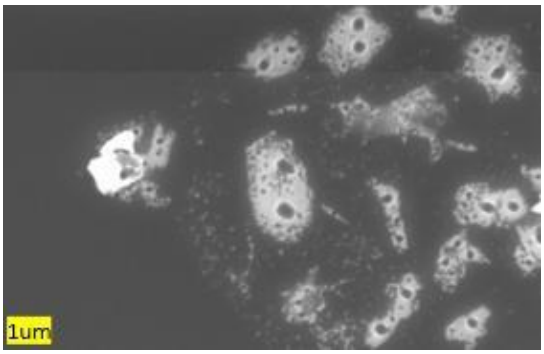

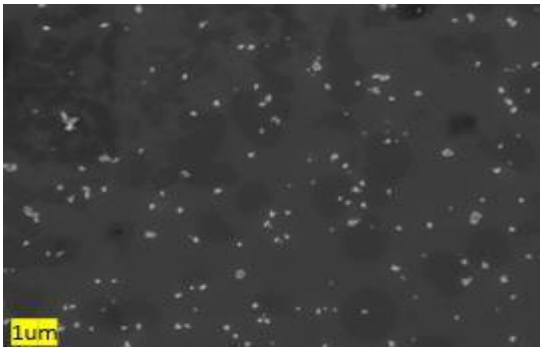

Fig 31.C ***Fig31.D***

Fig.31 Junk on the Substrate

We suspected that the junk was formed during the initial sample preparation step, with probable sources being listed below

- Tweezer
- Cooling liquid used during Dicing
- Residual Acetone on Substrate reacting with ozone in the UV-Ozone chamber

To solve the issue, we examined the Samples Under SEM in each cleaning step and developed a procedure to get a smooth and clean substrate, which is discussed below.

- **<u>Contamination source -tweezer</u>**

Tweezer had the least possible chances of introducing junk of this magnitude on the Si substrate, yet as a precautionary measure, and to avoid any probable contamination from the tweezer, we cleaned the tweezer every time before use with ethanol.

- **Contamination source cooling liquid used in the Dicing saw**

Initially, we thought that the cooling liquid used by the dicing saw one of the most probable causes for the formation of junk on the Substrate. To avoid this junk, the sacrificial SiO_2 was etched by parts using 10:1HF instead on a single go; by doing so, we ensured that the junk was not settled on top of the Silicon substrate.

- **Residual acetone /IPA reacting the UV-Ozone chamber**

The most prominently suspected cause for the junk formation was residual Acetone or IPA reacting up in the UV-Ozone chamber; to overcome this issue, a set of sample cleaning procedures was tried as mentioned in the table4 below. After cleaning the sample with each process, we observed those Si substrates under the SEM

Sample number	Pre-Uv Ozone treatment	Post Uv Ozone treatment
1	Hf etching of sacrificial SiO_2	IPA sonication
2	Hf etching of sacrificial SiO_2	IPA sonication followed by Di sonication, then IPA sonication
3	Hf etching of sacrificial SiO_2 +Acetone sonication +IPA sonication	Acetone Sonication followed by IPA sonication followed by Di sonication, then IPA sonication
4	Hf etching of sacrificial SiO_2	Acetone Sonication followed by IPA sonication followed by Di sonication, then IPA sonication

Table 4. Sample cleaning procedures

Results

Sample condition 1

The Si substrate was first etched in parts by using 10:1 HF. Then, the UV-ozone treatment of the bare Si substrate with UV-Ozone grows hydroxyl terminations on the Substrate, followed by IPA sonication.

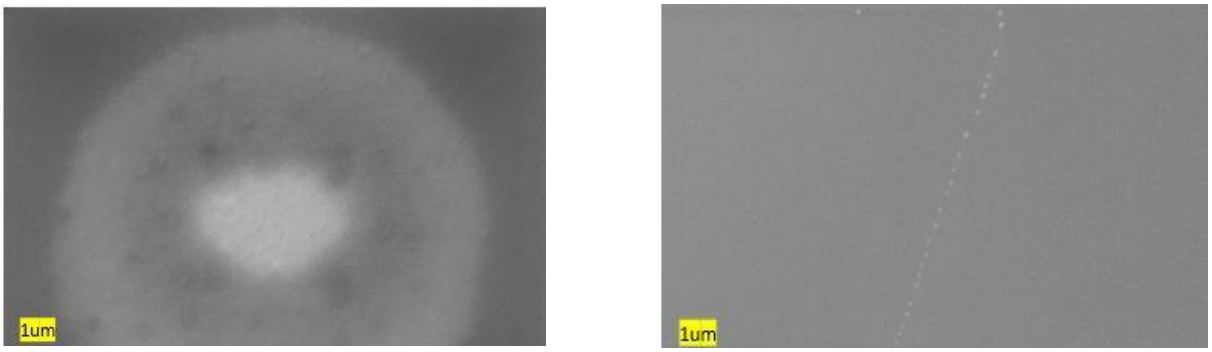

Fig32-Sample cleaned with HF+UV-O3+IPA sonication

Sample condition 2

The Si substrate was first etched in parts by using 10:1 HF, then by treating the bare Si substrate with UV-Ozone. The UV-ozone treatment grows hydroxyl terminations on the Substrate followed by IPA sonication, then sonication in DI and IPA again.

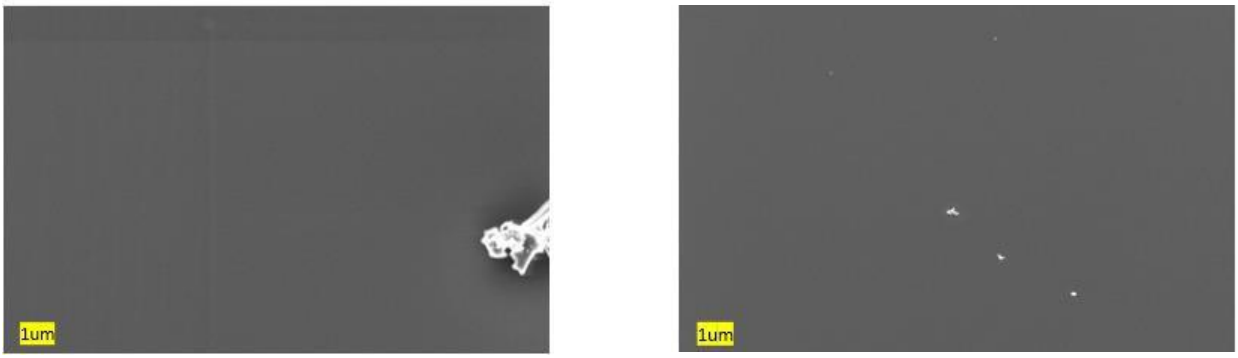

Fig33-Sample cleaned with HF+UV-O3+IPA +DI + IPA sonication

Sample condition 3

The Si substrate was first etched in parts using 10:1 HF. after etching the sacrificial oxide, and we sonicated the sample in Acetone followed by IPA.

Then treated the bare Si substrate with UV-Ozone the UV-ozone treatment grows hydroxyl terminations on the Substrate, followed by IPA sonication, then sonication in DI and IPA again.

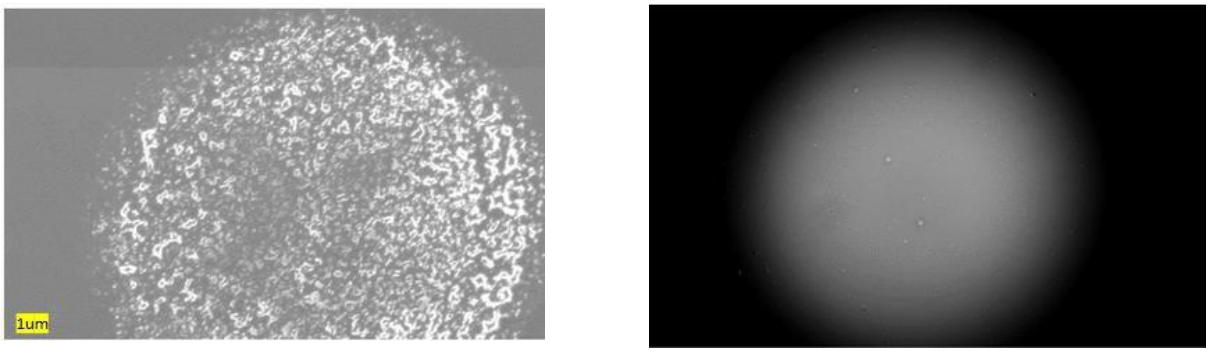

Fig34-Sample cleaned with HF+ Acetone+ IPA sonication +UV-O3+ Acetone+ IPA +DI+ IPA sonication

Sample condition 4

The Si substrate was first etched in parts using 10:1 HF. after etching the sacrificial oxide; the bare Si substrate was treated with UV-Ozone. The UV-ozone treatment grows hydroxyl terminations on the Substrate followed by Acetone sonication, then IPA sonication and sonication in DI and IPA again.

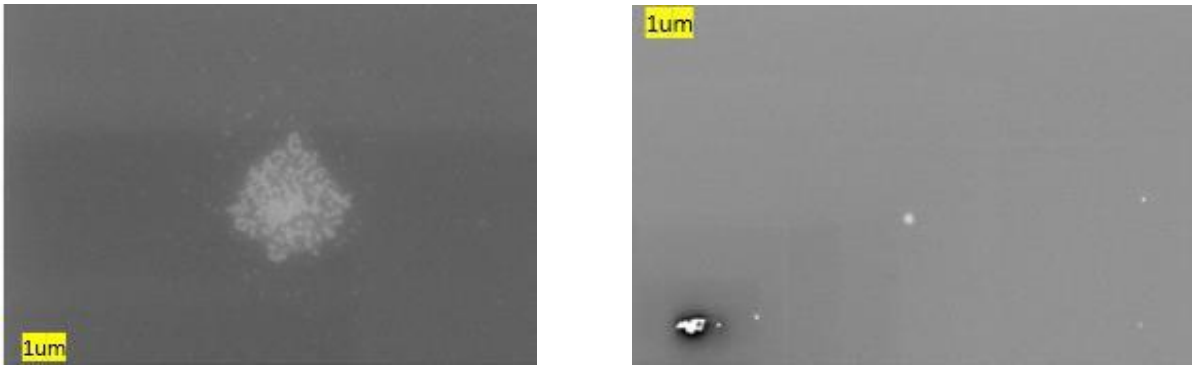

Fig35-Sample cleaned with HF UV-O3+ Acetone+ IPA +DI+ IPA sonication

Inference

After observing the SEM images in Fig. 32,33,34, and35, we found that Sample condition 2 gave the cleanest Si substrate. Further, the SEM images also made it clear that the acetone sonication introduced the majority of the junk on the Substrate. We found that Di sonication made the sample cleaner by comparing the SEM images in Fig 32 and 33.

Following cautions were also taken while cleaning the Substrate cleaning to avoid any contamination from any type of source

1. The Substrate had approximately 100 nm of thermally grown sacrificial SiO_2
2. After Dicing, the SiO_2 was etched in parts by using 10:1 HF (this ensured that no junk settled on the bare Si Substrate)
3. The UV Ozone chamber was per-cleaned with IPA and had an empty UV ozone run for 15 minutes (to avoid any carbon build-up)
4. It was ensured that the tweezer was with Di water and ethanol cleaned every time before use

5. The Glass beakers used for sonication always had less than three samples to avoid any cross-contamination from the samples
6. These beakers were properly cleaned before every sonication with IPA solution

4.5 Uneven C50 Placement

The second persistent issue observed in the SEM images was the uneven placement of C50.this uneven placement of C50 included agglomerations odf C50 as seen in SEM image in Fig.36a and fig36c. Uneven placement of C50 shown in SEM image of fig 36B and, Direct attachment of P30 on the substrate with a lot of P-30 agglomerations after passivation of APTES SAMs layer as seen in Fig 36a and fig36C on the Substrate, and a lot of P30 agglomeration

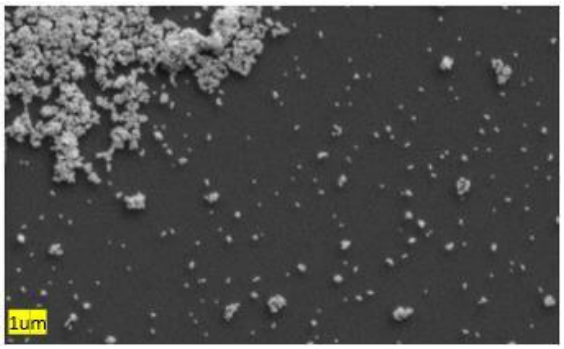

Fig.36a

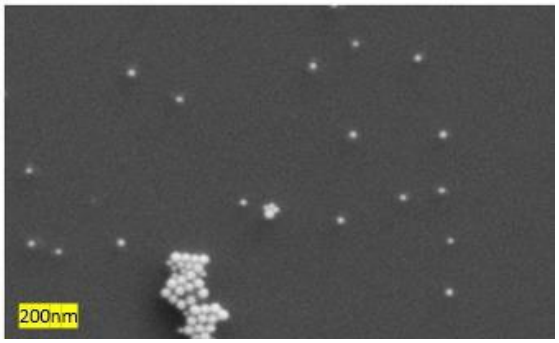

Fig.36B

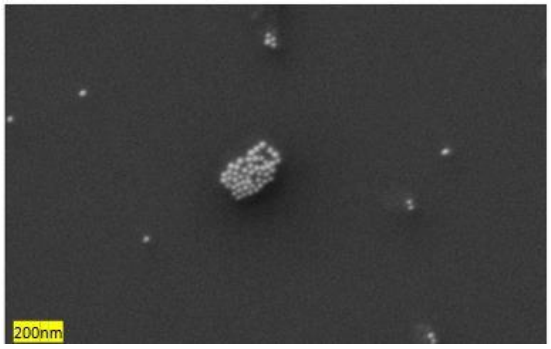

Fig36C

Fig.37-a) agglomeration ofP30 and attachment of P30 on substrate b) non-uniform placement of C50 c) Agglomerations of C30

All these issues indicated to one probable source, i.e., uneven or improper growth of APTES layer on the Si substrate; to overcome this problem, we first zeroed down all possible factors affecting the APTES layer formation on Si substrate in our recipe, and they were:-

1. NaOH Concentration
2. APTES volume used
3. APTES Timing
4. Post APTES rinsing
5. 5 APTES bake out time and temperature

Out of this condition, the APTES bakeout time and temperature were fixed to 120^{o}C for 10 mins on a hot plate

All the remaining parameters made a combination of a total of 16 samples, as mentioned in the table5 below

A few variables were fixed while studying the APTES experiment, i.e., the Substrate used was a bare Si substrate cleaned with the new cleaning procedure mentioned in the previous chapter. In addition, NaOH volume was fixed to 30 µL.

After the formation of APTES, the sample was rinsed three times with pH-13 ethanol and then three times with pure ethanol. The post aptes rinsing was tested after baking samples on a hot plate at 120^0C for 10 mins.

After the Growth of APTES, the regular experiment was done by eliminating the target step. This was done to check the Behavior of APTES post passivation of positive charge. The table below shows details of all 16 possible samples:

Sample number	APTES Volume	APTES Time	NaOH Concentration	Post-APTES Rising
Sample 1	10 µL	5 min	1 M	yes
Sample 2	10 µL	5 min	1 M	no
Sample 3	10 µL	20 min	1 M	yes
Sample 4	10 µL	20 min	1 M	no
Sample 5	10 µL	5 min	0.1 M	yes
Sample 6	10 µL	5 min	0.1 M	no
Sample 7	10 µL	20 min	0.1 M	yes
Sample 8	20 µL	20 min	0.1 M	no
Sample 9	20 µL	5 min	1 M	yes
Sample 10	20 µL	5 min	1 M	no
Sample 11	20 µL	20 min	1 M	yes
Sample 12	20 µL	20 min	1 M	no
Sample 13	20 µL	5 min	0.1 M	yes
Sample 14	20 µL	5 min	0.1 M	no
Sample 15	20 µL	20 min	0.1 M	yes
Sample 16	20 µL	20 min	0.1 M	no

Table 5-APTES experimental conditions

- **SEM images of each sample condition**

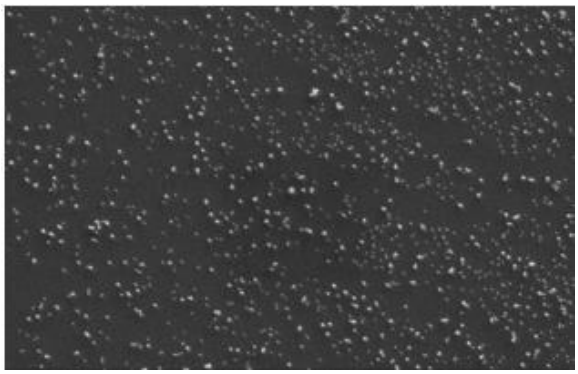

Fig.37A

Sample1:APTES:10ul-1MNaOH

All rinsing done in vortex

APTES time 5 minutes

Post APTES rinsing :Alternating low pH high pH wash with Squeeze Ethanol rinsing in between

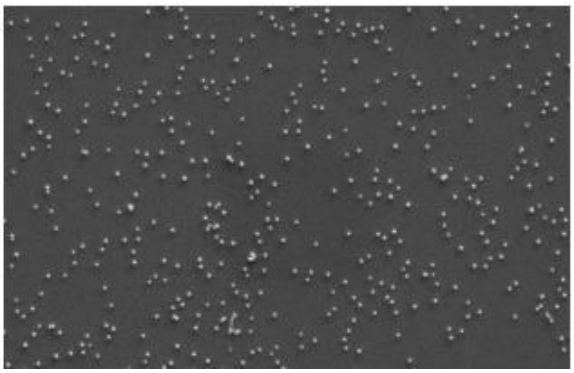

Fig.37B

Sample2:APTES:10ul-1MNaOH

All rinsing done in vortex

APTES time 5 minutes

Post APTES rinsing :NA

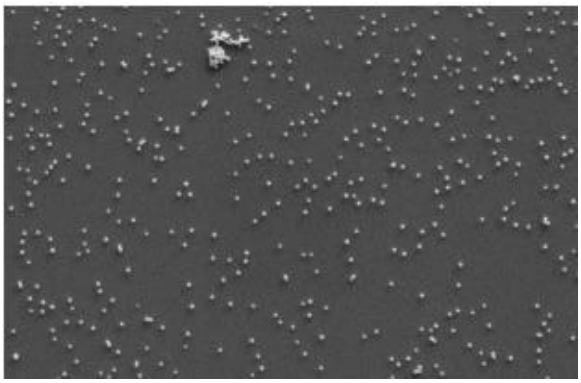

Fig.37 C

Sample1:APTES:10ul-1MNaOH

All rinsing done in vortex

APTES time 5 minutes

Post APTES rinsing :Alternating low pH high pH wash with Squeeze Ethanol rinsing in between

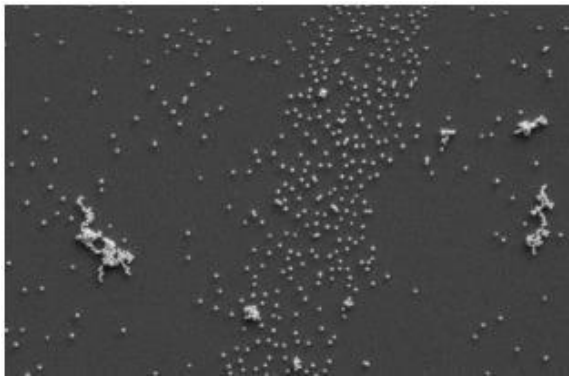

Fig.37 D

Sample2:APTES:10ul-1MNaOH

All rinsing done in vortex

APTES time 5 minutes

Post APTES rinsing :NA

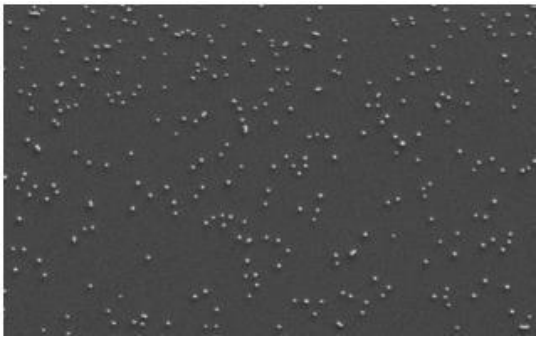

Fig.37E

Sample5:APTES:10ul;0.1MNaOH

All rinsing done in vortex

APTES time 5 minutes

Post APTES rinsing :Alternating low pH high pH wash with Squeeze Ethanol rinsing in between

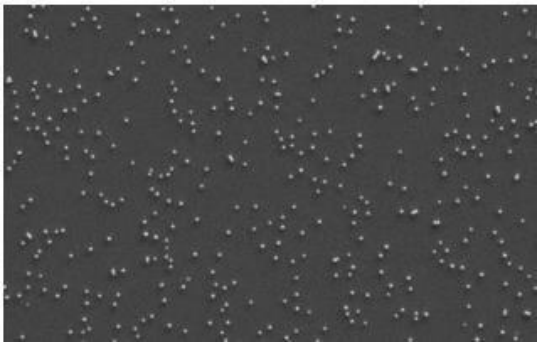

Fig.37F

Sample6:APTES:10ul;0.1MNaOH;

All rinsing done in vortex

APTES time 5minutes

Post APTES rinsing :NA

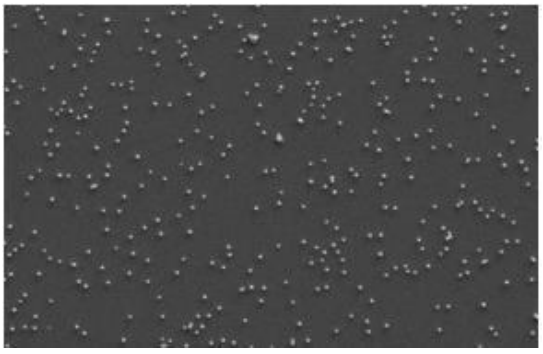

Fig.37G

Sample7:APTES:10ul;0.1MNaOH:

All rinsing done in vortex

APTES time 20 minutes

Post APTES rinsing :Alternating low pH high pH wash with Squeeze Ethanol rinsing in between

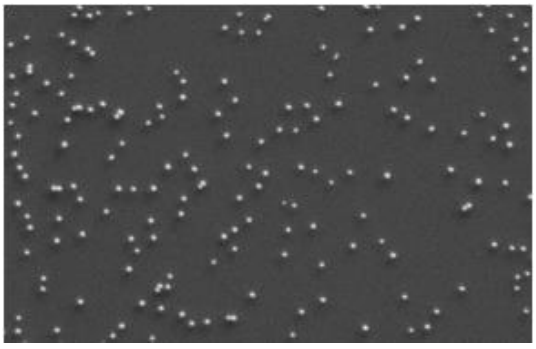

Fig.37H

Sample8:APTES:10ul;0.1MNaOH

All rinsing done in vortex

APTES time 5minutes

Post APTES rinsing :NA

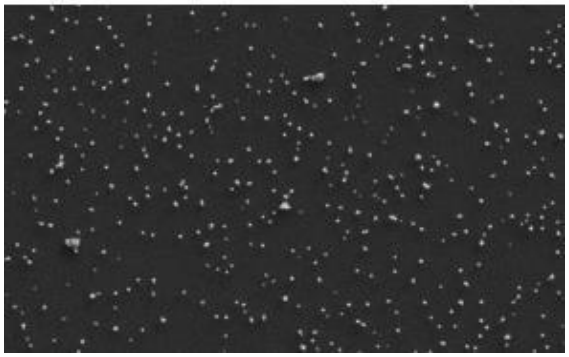

Fig. 37 I

Sample9:APTES:20ul;1MNaOH:30ul

All rinsing done in vortex

APTES time 5 minutes

Post APTES rinsing :Alternating low pH high pH wash with Squeeze Ethanol rinsing in between

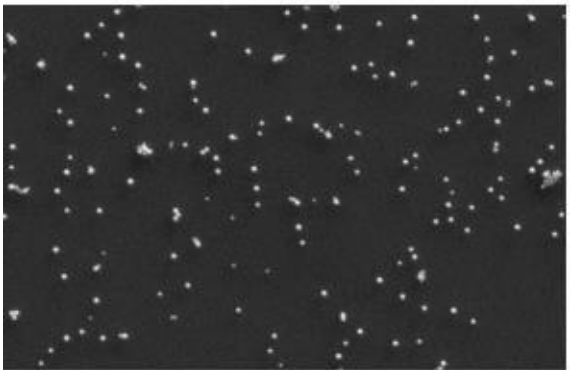

Fig. 37J

Sample10:APTES:20ul;1MNaOH;30ul

All rinsing done in vortex

APTES time 5minutes

Post APTES rinsing :NA

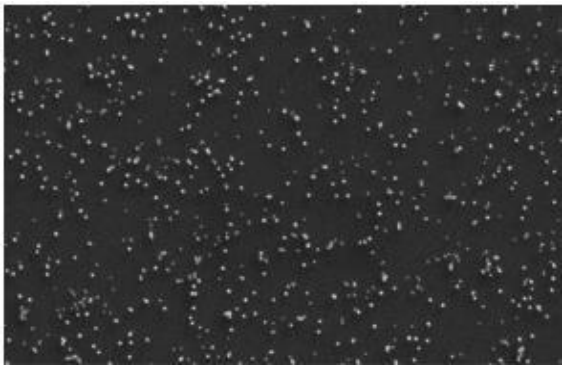

Fig. 37K

Sample11:APTES:20ul;1MNaOH:30ul

All rinsing done in vortex

APTES time 5 minutes

Post APTES rinsing :Alternating low pH high pH wash with Squeeze Ethanol rinsing in between

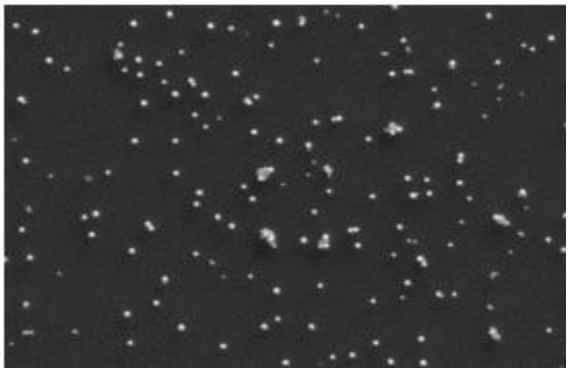

Fig. 37L

Sample12:APTES:20ul;1MNaOH;30ul

All rinsing done in vortex

APTES time 5minutes

Post APTES rinsing :NA

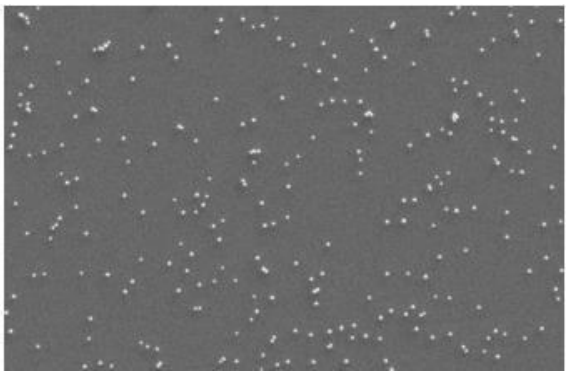

Fig.37M

Sample13:APTES:20ul;0.11MNaOH:30ul

All rinsing done in vortex

APTES time 5 minutes

Post APTES rinsing :Alternating low pH high pH wash with Squeeze Ethanol rinsing in between

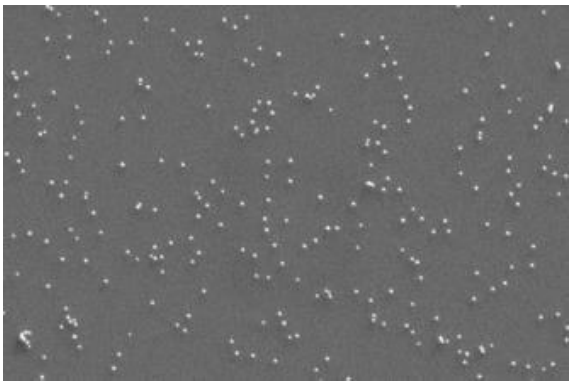

Fig.37N

Sample14:APTES:20ul;0.1MNaOH;30ul

All rinsing done in vortex

APTES time 5minutes

Post APTES rinsing :NA

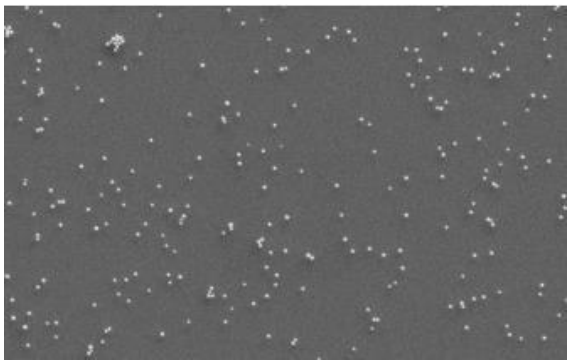

Fig.37O

Sample15:APTES:20ul;0.1MNaOH:30ul

All rinsing done in vortex

APTES time 20 minutes

Post APTES rinsing :Alternating low pH high pH wash with Squeeze Ethanol rinsing in between

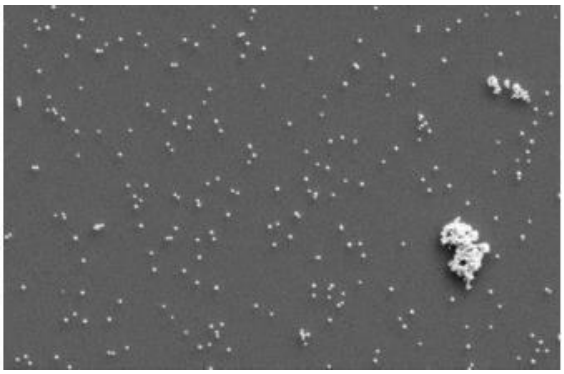

Fig.37P

Sample16:APTES:20ul;0.1MNaOH;30ul

All rinsing done in vortex

APTES time 20minutes

Post APTES rinsing :NA

F ig 37 Atop all SEM images for APTES experiment

Inference:

After observing the SEM images for all the sample conditions listed in in fig 37, we can infer that

- The Samples with 0.1 M NaOH solution in APTES has denser and even placement of C50 on the Substrate
- Using 30µL of 1M NaOH had no center attachments, but all the nanoparticles were attached at the edge of the spot area
- Using 10 µL of APTES solution has minimal or no P30 attachment on the Substrate
- Use of 10 µL of APTES solution also has minimal or no C50 agglomeration
- Both 5 minutes and 20 minutes for the formation of APTES gives APTES layer on the SUBSTRATE with 20 minutes APTES timing being more uniform
- The sample without rinsing has better Results than the one rinsed after
- Considering all the conclusions stated above, we thus establish a new recipe for the formation of APTES as follows

APTES Volume: 10 µL

NaOH Concentration:0.1M NaOH

NaOH volume: 30 µL

APTES timing: 20 minutes without any post APTES rinsing

This recipe gives a robust and uniform placement of C50

4.6 Improper and inconsistent satellite structure formation

So far, we were having issues forming a uniform and saturated satellite structures that we suspected were due to problems like uneven APTES formation and junk on Substrate. We addressed these issues individually and optimized those processes. However, we still were not able to establish a robust procedure for forming satellite structures. Predominantly we were having two major problems now, and they were

1. **<u>Uneven or no attachment of P30 on the C50</u>**

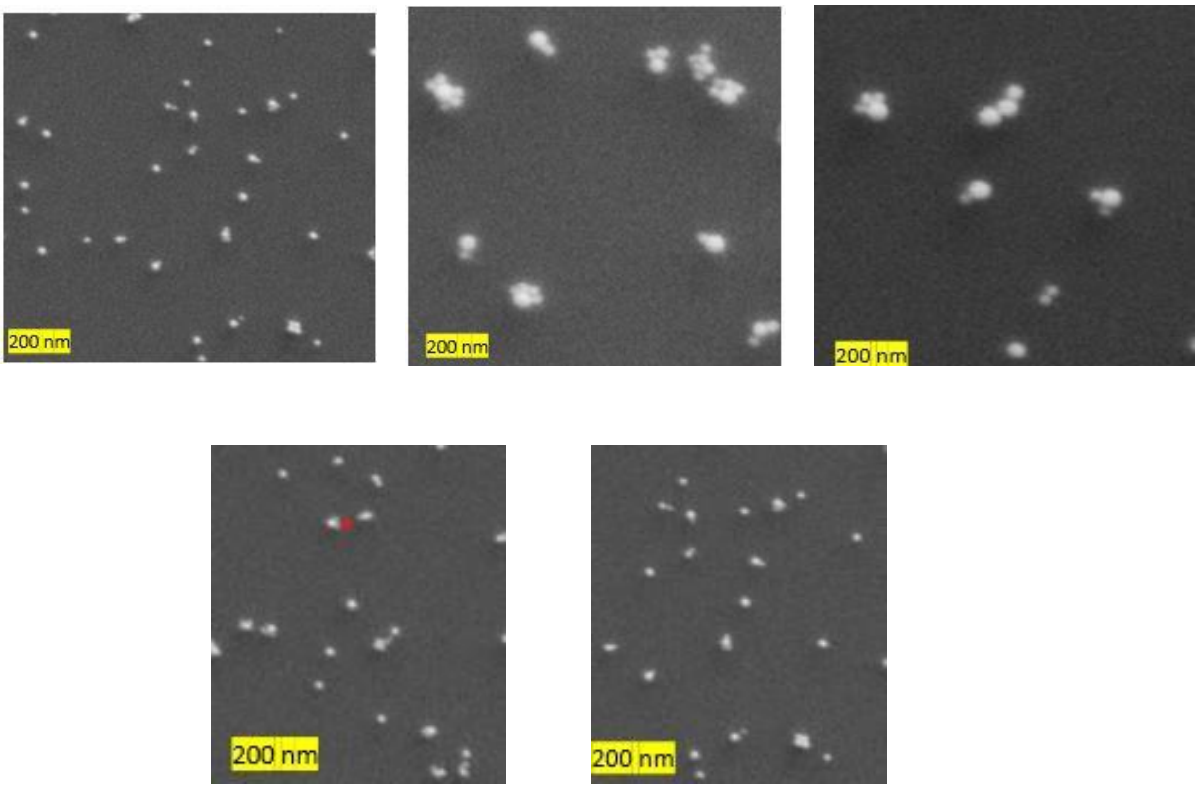

Fig38 Sem images showing Uneven P30 attachment

We could see in the SEM images from figure 38 that there were hardly any P30 attached to the C50. This indicated that there is not enough room for the target to hybridize with the C50, and there is no p30 hybridization.

2. Detachment of P30

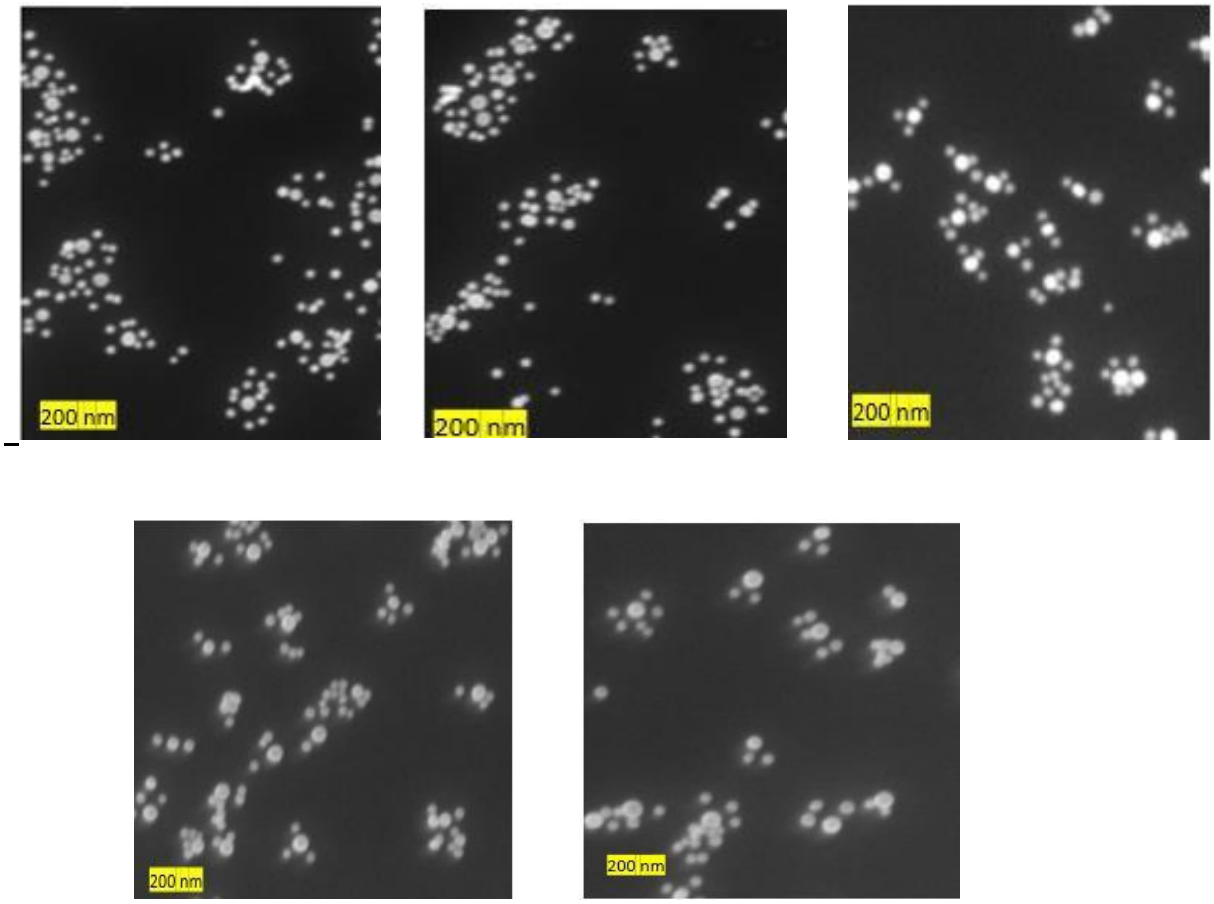

Fig39 Sem images showing P30 detachment

The Detachment of P30 indicated that target and p30 hybridization initially broke off either due to weak binding or breaking of bonds.

We address both these issues in the next section

4.5 Use of Spacer DNA

Improper and uneven satellite structures still were not addressed. To find the root cause of this problem, when we analyzed our data, we found that there was not enough room for the target to hybridize with capture DNA, which caused improper/week hybridization. The target was not having enough room for attachment because of the high density of DNA on nanoparticles. In the previous chapter, we saw that the Nanoparticles survived 2M NaCl, this was a clear indicator of a high density of DNA loaded on the nanoparticles. To overcome this issue, we introduced spacer DNA of Adenine; as discussed in the background section, Adenine would reduce the density of DNA on nanoparticles.

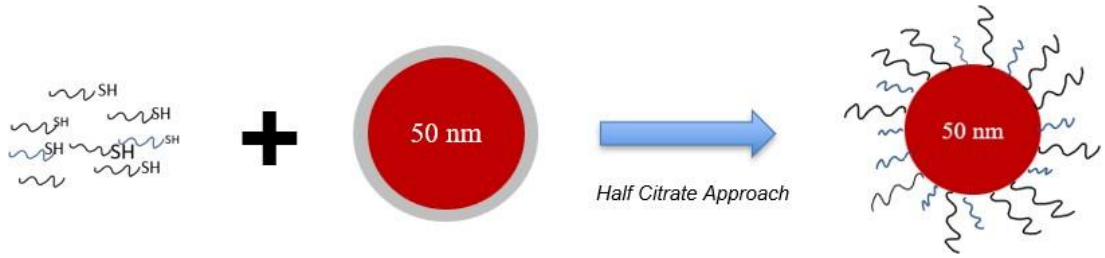

Fig 40.Schematic representation for Capture + Spacer conjugation

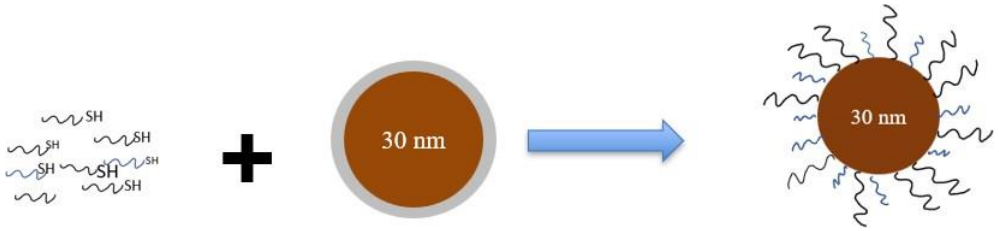

Fig 41.Schematic representation for probe + Spacer conjugation

The DNA conjugation method remains the same, slightly changing the mixing procedure. The purified DNA with all the buffers is mixed in the nanoparticles with rapid mixing. The schematic Fig 40 and 41 above shoes the conjugation process

The Hybridization conditions while exploring the use of spacer and DNA strands of different lengths were fixed as

- Hybridization buffer concentration-4XSSPE
- Hybridization temperature-50^{o}C
- Hybridization abuffer and stringency washing buffer made out of SDS
- Samples were cleaned with new cleaning procedure.
- APTES growth on Si substrate was done with the newly established recipy.

- **<u>DNA and Spacer length A7</u>**

We started with the spacer DNA of length A7i.e 7 bases of Adenine and tried various DNA to spacer ratios as mentioned in table 6 below ; the DNA sequence we used is as follows.

- Capture DNA sequence

TTTGCGGCCAATGTTTGTAAAAAAAAAAAA

- Probe DNA sequence

AAAAAAAAAAGCGCGACATTCCGAAGAA

- Spacer sequence

AAAAAAA

Capture DNA: Spacer DNA	Probe DNA: Spacer DNA Combinations
1:1	1:1,1: 3,1, 3:1,4:1,9:1
1:3	1:1,1: 3,1, 3:1,4:1,9:1
9:1	1:1,1:3,9:1

Table 6: Capture: Spacer ratio and Probe: Spacer ratio combinations

- **SEM Results**

As mentioned earlier, the spacer was used to make room for t-DNA to hybridize with, C-AuNP and , P-AuNP. The primary intention of using spacer DNA of length A7 was to check whether adding spacer DNA could give an excellent P30 attachment and form some structures. Furthermore, find the best possible combination of C/P-DNA and spacer DNA.

Capture: Spacer=>1:1 & Probe: Spacer=>1:1,1:3,1:4,9:1

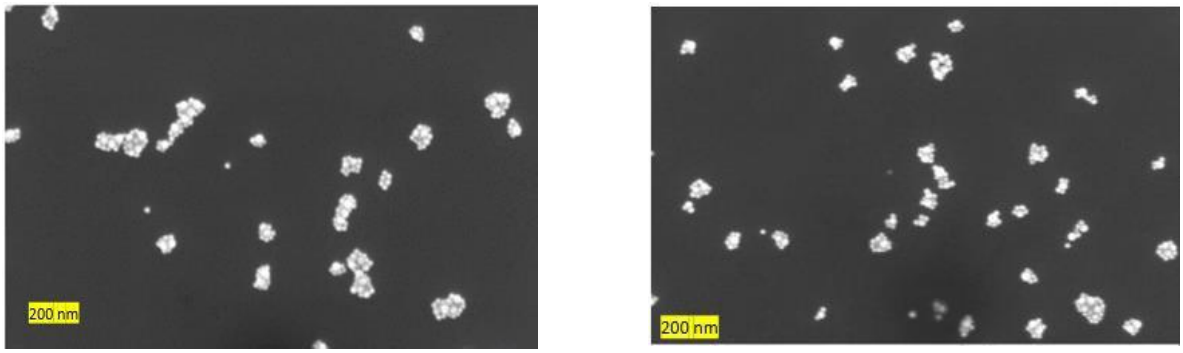

Fig.42 A Spacer a7- c: Spacer 1:1 P: Spacer 1:1

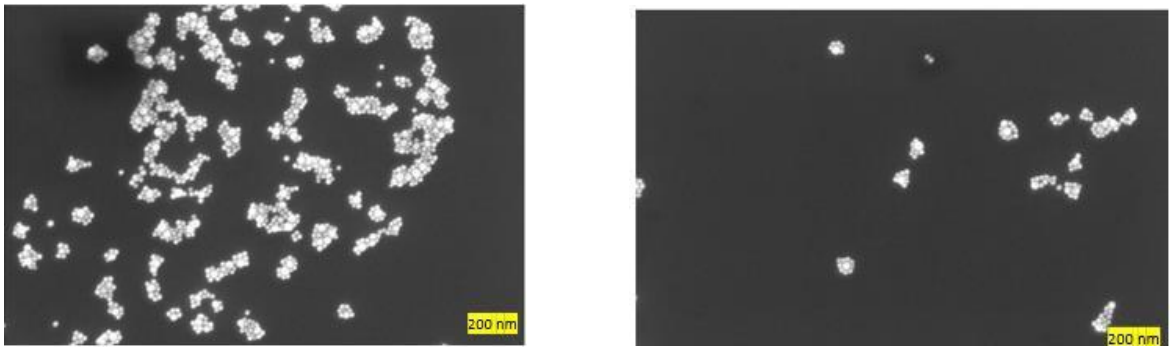

Fig.42 b Spacer a7- c: Spacer 1:1 P: Spacer 3:1

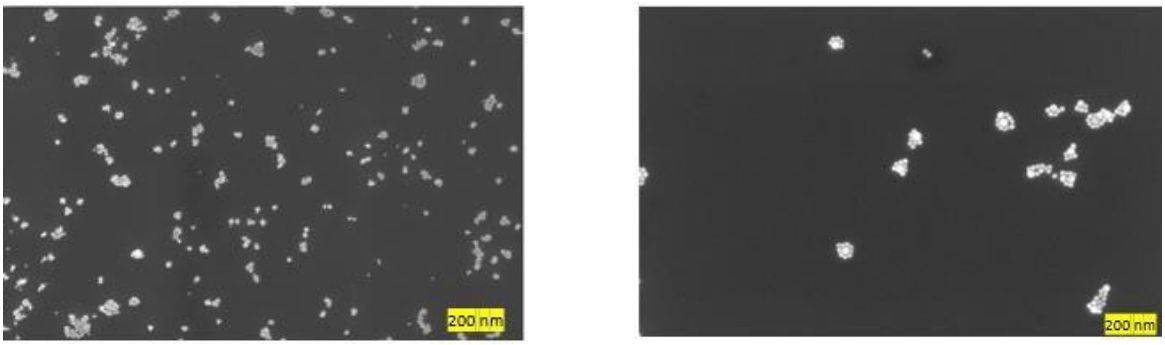

Fig.42 c Spacer a7- c: Spacer 1:1 P: Spacer 4:1

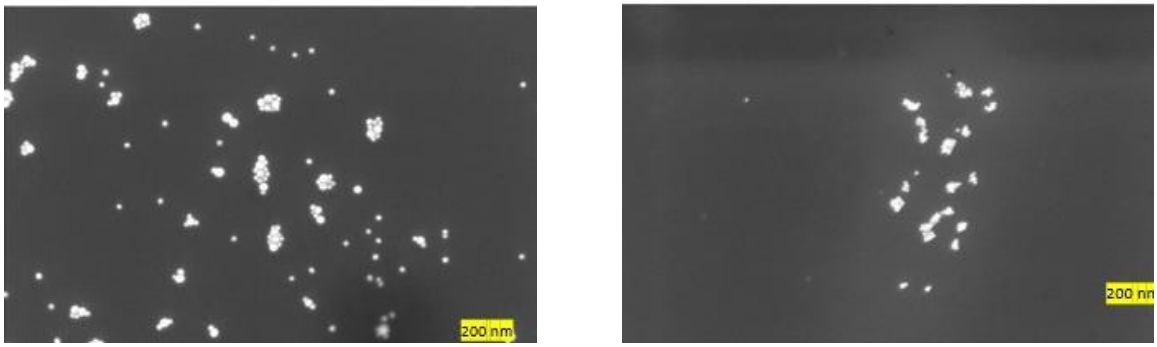

Fig.42 d Spacer a7- c: Spacer 1:1 P: Spacer 9:1

Capture: Spacer=>1:3 & Probe: Spacer=>1:1,1:3,4:1,9:1

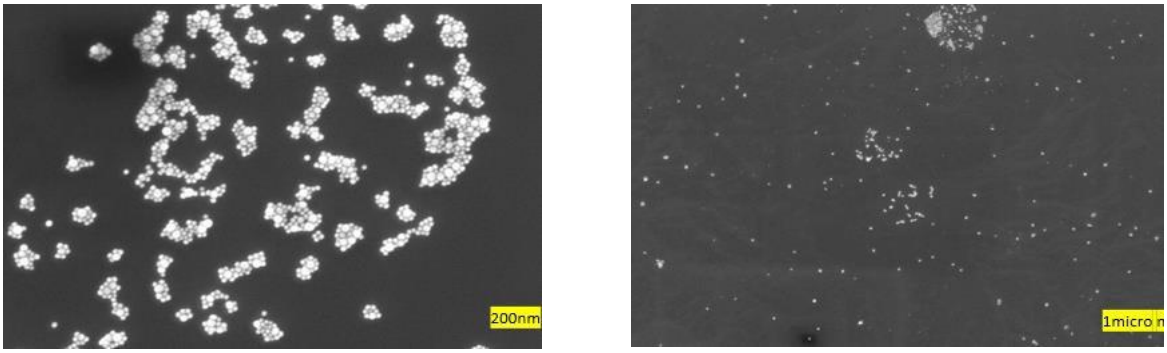

Fig.43 A Spacer a7- C/Spacer 1:3 P/ Spacer 1:1

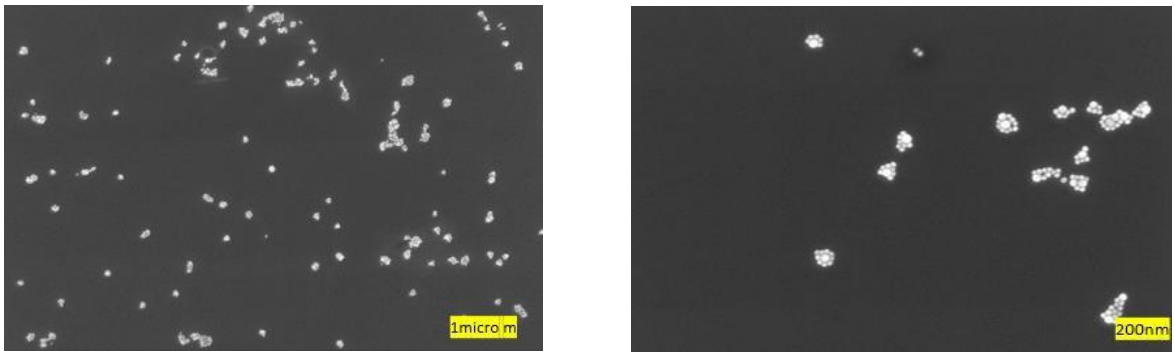

Fig.43 B Spacer a7- C/Spacer 1:3 P: Spacer 1:3

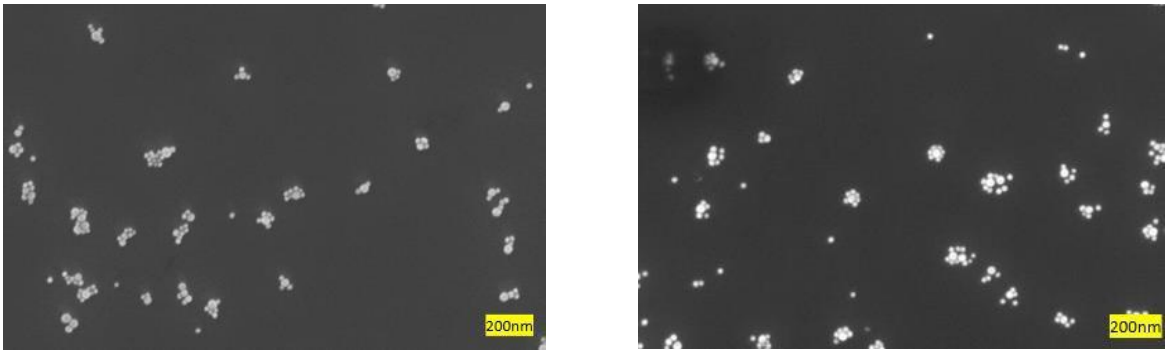

Fig.43 BcSpacer a7- c: Spacerf1:3 P: Spacer 4:1

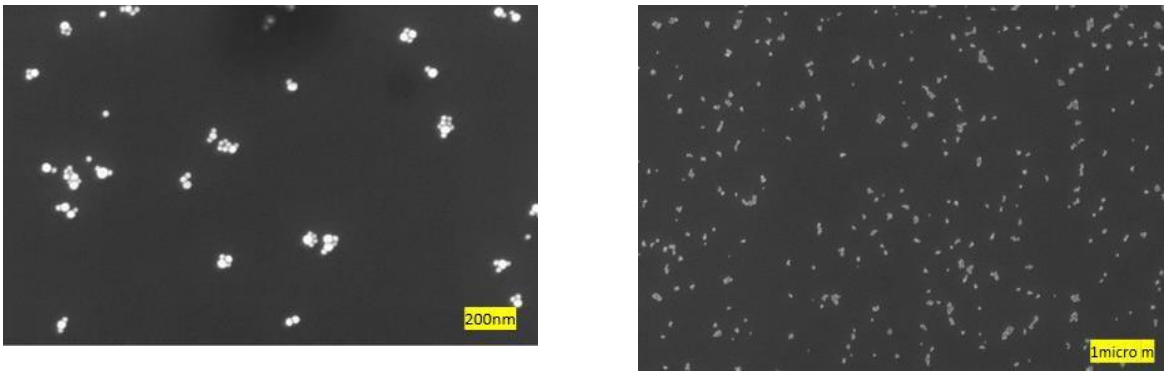

Fig.43 D Spacer a7- C/Spacer 1:3 P/ Spacer 9:1

Spacer and DNA length A7Capture: Spacer=>9:1 & Probe: Spacer=>1:1,1:3,9:1

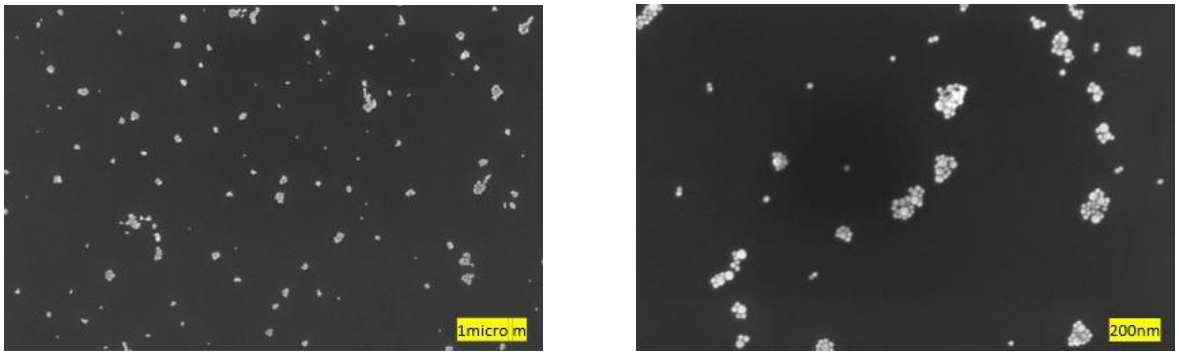

Fig.44 A Spacer a7- C/Spacer 9:1 ; P/ Spacer 1:1

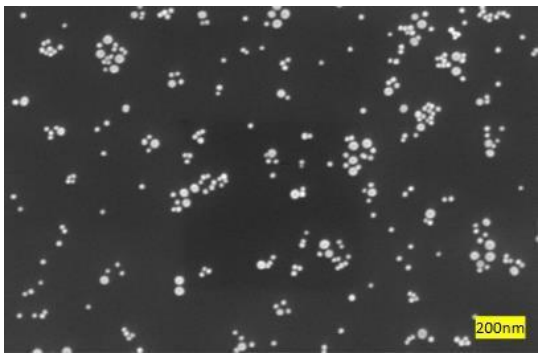

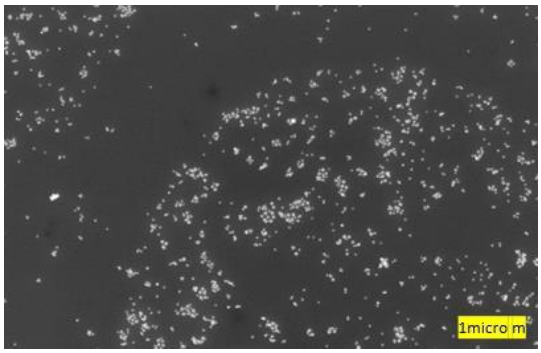

Fig.44 B Spacer a7- C/Spacer 9:1 P: Spacer 1:3

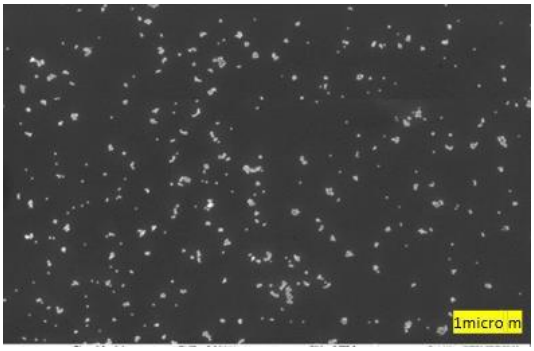

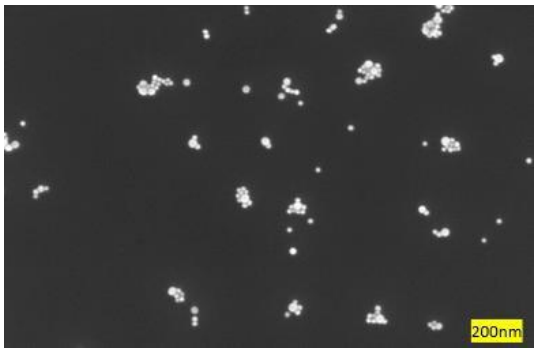

Fig.44 B Spacer a7- C/Spacer 9:1 P/Spacer 9:1

Inference

It is clear from the SEM Images in fig.42 to 44 that the use of Spacer DNA has improved the P30 attachment on CAuNP's. We could see the formation of satellite structures for a few combinations of capture/Spacer ratio and Probe/Spacer ratio. We could also see a trend in all the combinations tried that a higher number spacer or C& P DNA had very few attachments.Though we had P-30 attache on C-AuNP's these attachment and satellite structure formations were not consistent and reproducible at all .

- **DNA and Spacer length-A18**

As established in the previous chapter, we saw that the use of spacer resulted in a good amount of attachment of P30. Nevertheless, these structures were not at all consistent. To get more consistency in our results, we decided to use even longer DNA strand with the idea that longer DNA will provide more room for the Target to hybridize with the captured DNA and further with Probe. Considering the inference from the previous section, we explored the following combinations of Capture to spacer and Probe to the spacer

Capture DNA: Spacer DNA	Probe DNA: Spacer DNA Combinations
1:1	1:1,3:1,1:3
1:3	1:1,3:1,1:3

Table7 ***Capture: Spacer ratio and Probe: Spacer ratio combinations for DNA length A18***.

The C-DNA, P-DNA, Spacer sequence are as follows

- Capture DNA

TTTGCGGCCAATGTTTGTAAAAAAAAAAAAAAAAAAAA

- Probe DNA

AAAAAAAAAAAAAAAAAAAAGCGCGACATTCCGAAGAA

- Spacer DNA

AAAAAAAAAAAAAAAAA

- **SEM Results**

Spacer and DNA length -A18; Capture: Spacer=>1:1 & Probe: Spacer=>1:1,1:3,3:1

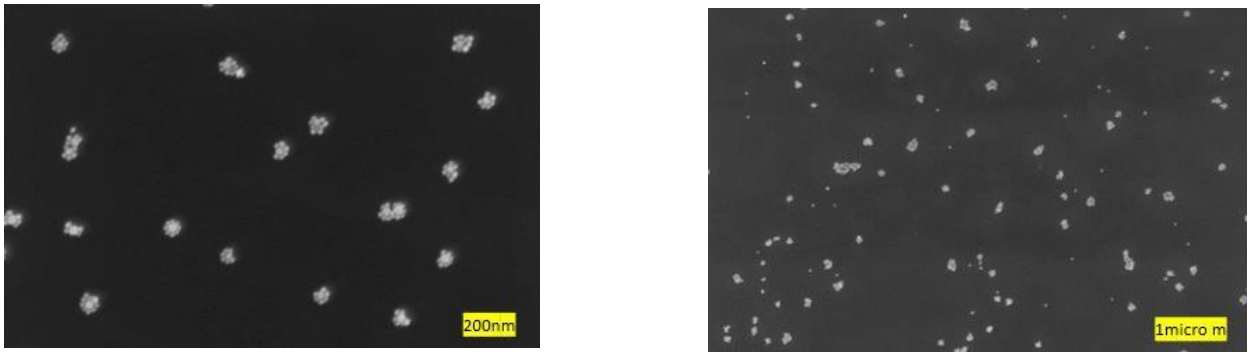

Fig.45 A Spacer a18- c: Spacer 1:1 P: Spacer 1:1

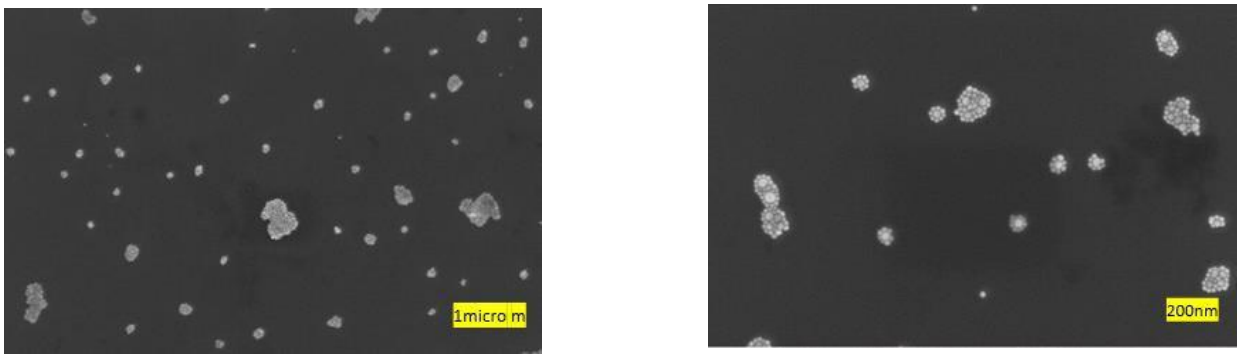

Fig.45 B Spacer a18- c: Spacer 1:1 P: Spacer 1:3

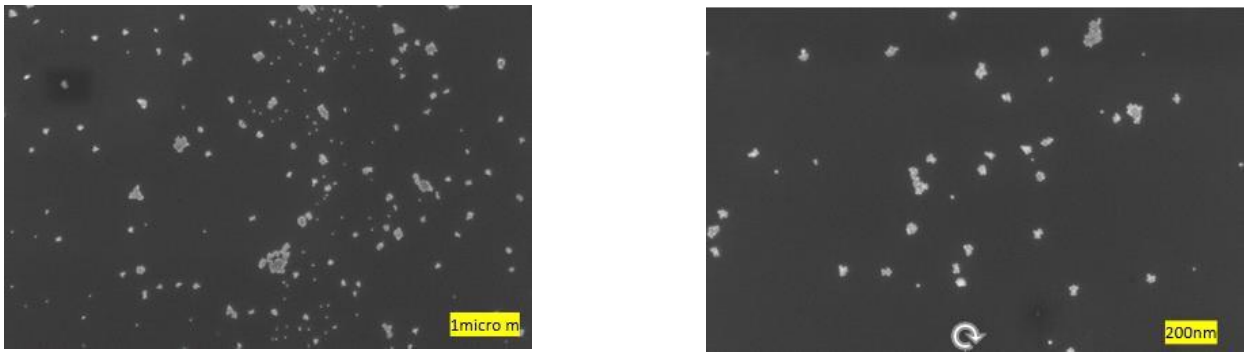

Fig.45 c Spacer a18- c: Spacer 1:1 P: Spacer 3:1

Spacer and DNA length -A18; Capture: Spacer=>1:3 & Probe: Spacer=>1:1,1:3,3:1

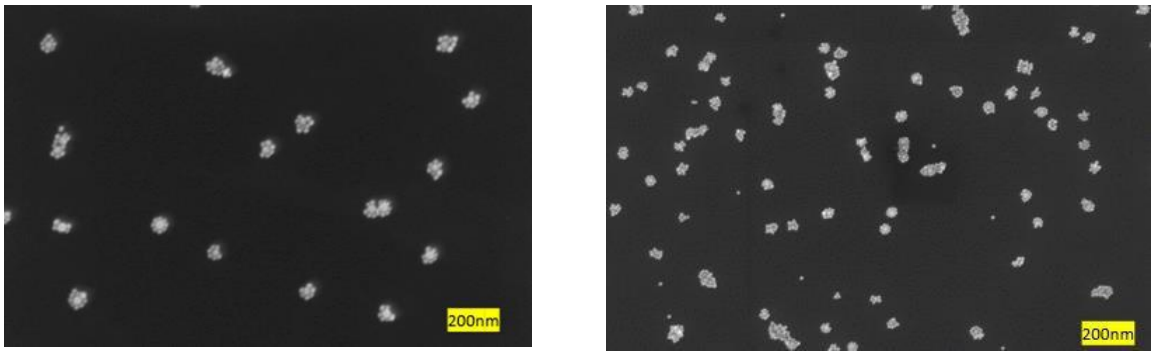

Fig.46 A Spacer a18- c: Spacer 1:3 P: Spacer 1:1

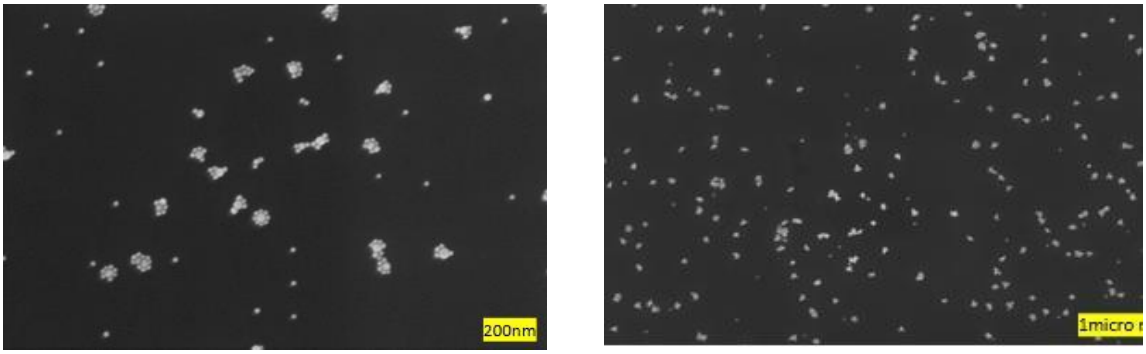

Fig.46 B Spacer a18- c: Spacer 1: P: Spacer 1:3

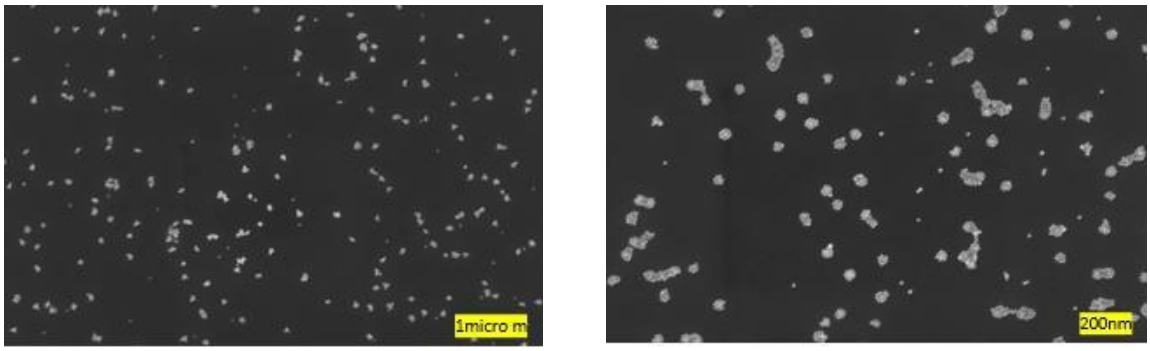

Fig.46 c Spacer a18- c: Spacer 1:3 P: Spacer 3:1

- **Inference**

Using a longer Spacer and C/P DNA gave a good amount of attachment. The satellite structures were reproduced multiple times.

- **DNA length A28**

The previous section clarified that DNA with A18 gave enough room for the target and P-DNA to bind with the Capture DNA. While the A18 DNA gave enough room for attachment, but it was not robust as the Capture DNA was not fully saturated. With an idea to create more room for the target to hybridize with the capture DNA, an even longer DNA strand of length A28 was conjugated with the AUNP the length of spacer DNA it was still fixed at A18. Table9 below shows all the combinations of C-DNA/spacer and P-DNA/spacer used.

Capture DNA/Spacer DNA combinations	Probe DNA/Spacer DNA Combinations
1:1	1:1,2:1,3:1
1:2	1:1,2:1,3:1
1:3	1:1,2:1,3:1

Table9 ***Capture: Spacer ratio and Probe: Spacer ratio combinations for DNA length A28***

The DNA sequence of capture DNA and probe DNA that were used in these combinations are listed below . The Spacer DNA sequence was the same as the one used for DNA with length A18

- Capture DNA

TTTGCGGCCAATGTTTGTAAAAAAAAAAAAAAAAAAAAAAAAAAAA

- Probe DNA

AAAAAAAAAAAAAAAAAAAAAAAAAAAAGCGCGACATTCCGAAGAA

- **SEM Results**

Spacer length A18 and DNA length -A28; Capture: Spacer=>1:1 & Probe: Spacer=>1:1,2:1,3:1

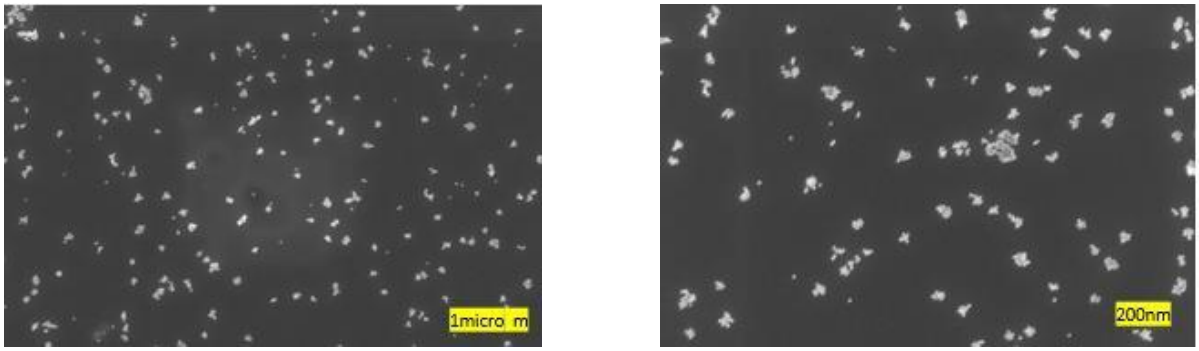

Fig.47 a-DNAa28/ Spacer a18- c: Spacer 1:1 P: Spacer 1:1

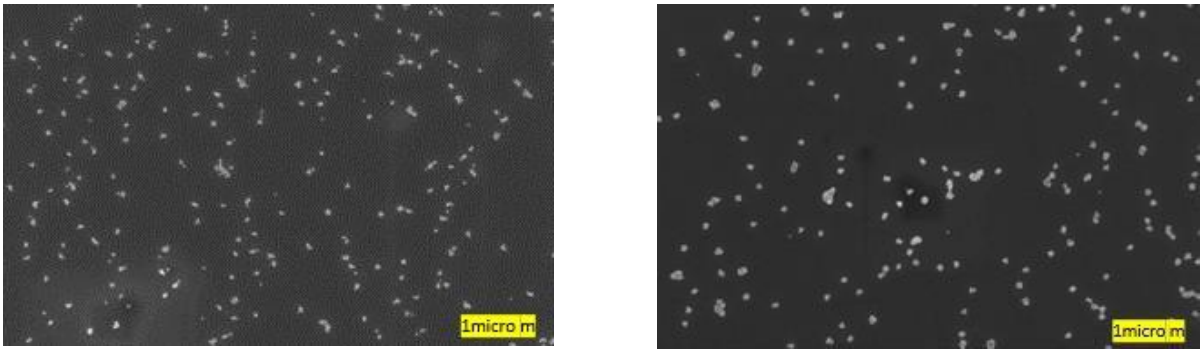

Fig.47 B-DNAa28/ Spacer a18- c: Spacer 1:1 P: Spacer 1:3

Spacer length A18 and DNA length -A28; Capture: Spacer=>2:1 & Probe: Spacer=>1:1,2:1,3:1

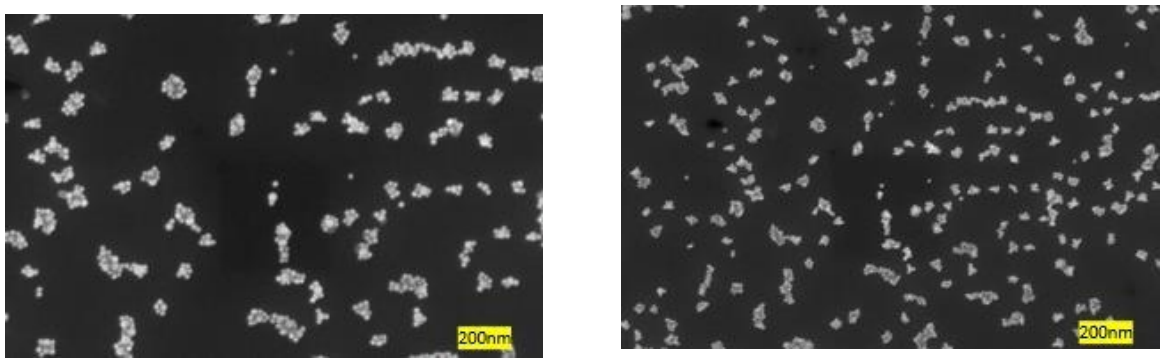

Fig 48 **A-DNAa28/ Spacer a18- c: Spacer 1:1 P: Spacer 1:3**

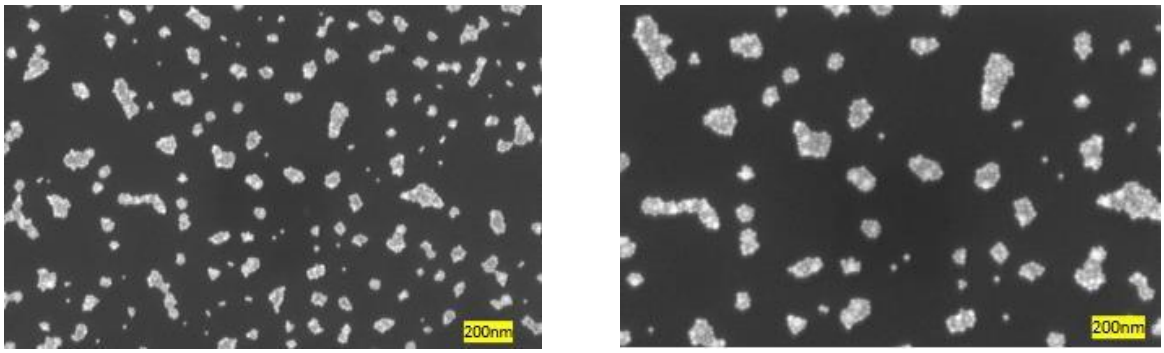

Fig.48 **B-DNAa28/ Spacer a18- c: Spacer 1:1 P: Spacer 1:3**

- **Inference**

Using an even longer DNA gave more attachment of P30 on C50, with the majority of C50 having saturated satellite structures. This procedure was robust and reproducible. Further, when

we compared the nanostructures formed with Different DNA and spacer length, we were able to establish a trend that a longer had a better attachment

4.6 Detachment of P30

The other issue that we saw was detachment of P30 as shown in SEM images of Fig.52 . The detachment of P30 can be seen as an extension to the uneven attachment of P30. Detached P30 indicated that the target and P30 were initially hybridized but detached from the C50 either in the stringency washing or during sample cleaning after post-stringency washing. This detachment was occurring probably due to two reasons. Either the target and P30 were weekly bounded to the C50, or the residual hybridization buffer left on the Substrate broke the uniformly attached target and p30 from the C50.

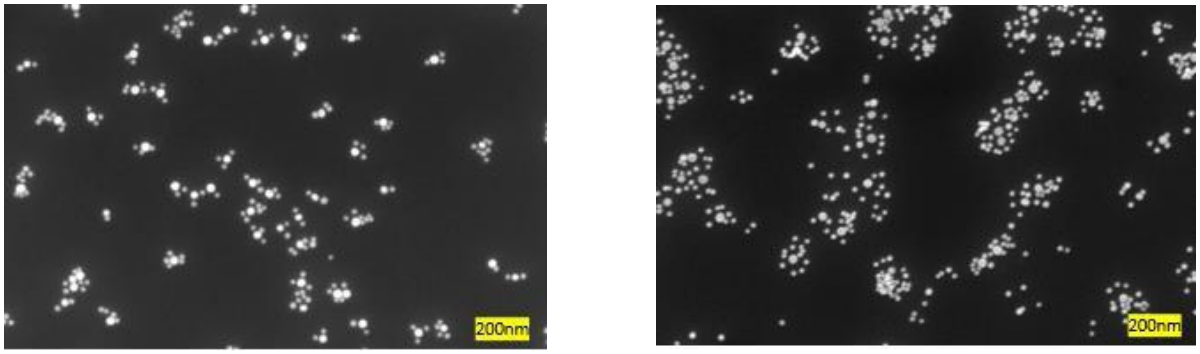

Fig.52 Detachment of P30

The first of the two probable causes of week hybridization was addressed by using a longer DNA and a spacer DNA. It gave more room for the target to bind with the C50 eliminating the possibility of weak binding. The second probable cause of detachment was the residual stringency

washing buffers, as the samples were naturally dried post P30 stringency washing. There was a high probability of residual buffer to remain on the Substrate.

To overcome this problem, it was necessary to get rid of the buffer without damaging the newly formed nanostructures .to get rid of the residual buffer without disturbing the nanostructures. Therefore, the sample was immediately dipped in an alcohol solution for a second and gently blow-dried with N_2 gas. To fine-tune this process, three alcohol solutions are Methanol, Ethanol, and IPA.

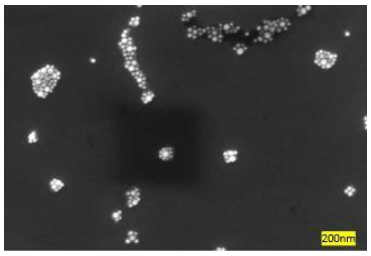

Fig52A-methanol Dip

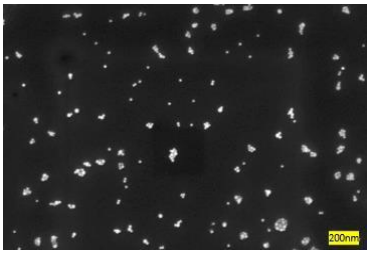

Fig 52 B ethanol Dip

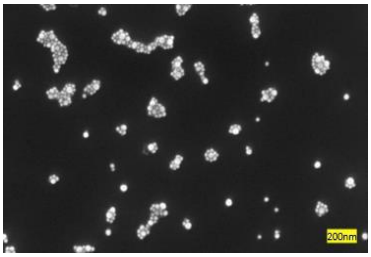

fig 52C IPA DIP

- **<u>Inference:</u>**

Looking at the SEM images in figure 52, it was clear that a quick dip in alcohol solution could easily eliminate residual stringency washing buffer. These images clearly showed that using IPA solution did not disturb the newly formed structures.

4.7 Target Extraction Using MMP experiment

The main goal of this experiment is to extract the pure target DNA by using DNA functionalized Magnetic microparticles or MMP; this target extraction is a two-step process

1. **Attachment of Sulfo-SMCC to the amine-coated MMPs**
2. **Attachment DNA (S-H terminated) to Sulfo-SMCC/amine-coated MMP**

To achieve the first step of attachment of Sulfo-SMCC to the amine-coated MMP's we follow the procedure listed below:

- We Prepare 1 mL of 5 mM Sulfo-SMCC in 1X Phosphate buffer saline (PBS) (pH 7.4; Sigma-Aldrich P5493-1L) and Heat at 50C for 1 minute
- Apply a strong magnet to the tube of 100 µL BioMagPlus Amine, take out supernatant, Add the 1 mL of 5mM Sulfo-SMCC; Mix well in a rotational shaker for 1 hour
- We purify the MMP-Sulfo SMCC colloid by applying a strong magnet to the tube wall and removing the supernatant.
- Add 1 mL 1X PBS, take out a magnet, and mix well
- Repeat the above step 3 times
- Apply a strong magnet to the tube wall, take out supernatant, add 300 µL 2X PBS, take out a magnet, and mix well

Once The MMP are purified, they are ready for attachment of DNA

Attachment DNA (S-H terminated) to Sulfo-SMCC/amine-coated MMP is done using the following procedure

- Mix 300 µL DNA (in DI) with the above 300 µL solution (Sulfo-SMCC/amine-coated MMPs in 2X PBS)
- Mix well in a rotational shaker for 4 hours.

The purification of the above colloid is done by using the following procedure: -

- Apply a strong magnet to the tube wall, take out supernatant,
- add 1 mL TE, take out a magnet and mix well·
- Repeat the above Step 4 times
- Store the colloid in the refrigerator

Target Extraction Using Magnetic Micro Particles

To demonstrate the Capture of target DNA by C-DNA and compare the yield with DNA/DI, we followed the following steps

3. Preparation of C-MMP

- Take out 100 µL of AC-MMP (8.3E-13 M in TE)
- Apply a magnet, take out the TE and add 200 µL 6X SSPE HB

4. Mix the target with AC-MMP

- The Target DNA has the sequence
- Add the above 200 µL AC-MMP (in 10X SSPE HB) to 10 µL target (10□1 M in TE)

- Incubate for 10 minutes in the vortex shaker at the lowest speed

5. Purification of colloid

- Apply a strong magnet to the tube wall, take out supernatant, take out the magnet, add 50 µL of 10X SSPE HB, mix well
- Repeat the above step 4 times

6. Extraction of target DNA

- Apply a strong magnet to the tube wall, take out supernatant, take out the magnet, add 10 µL DI, mix well for 10 minutes
- Apply a strong magnet to the tube wall, take out the supernatant for UV-VIS measurement

We compare Uv-Vis's measurements of the above-extracted target with target DNA in 1XPBS

(UV-Vis's measurements taken at absorbance 260nm as DNA absorbs light at a wavelength of 260 nm)

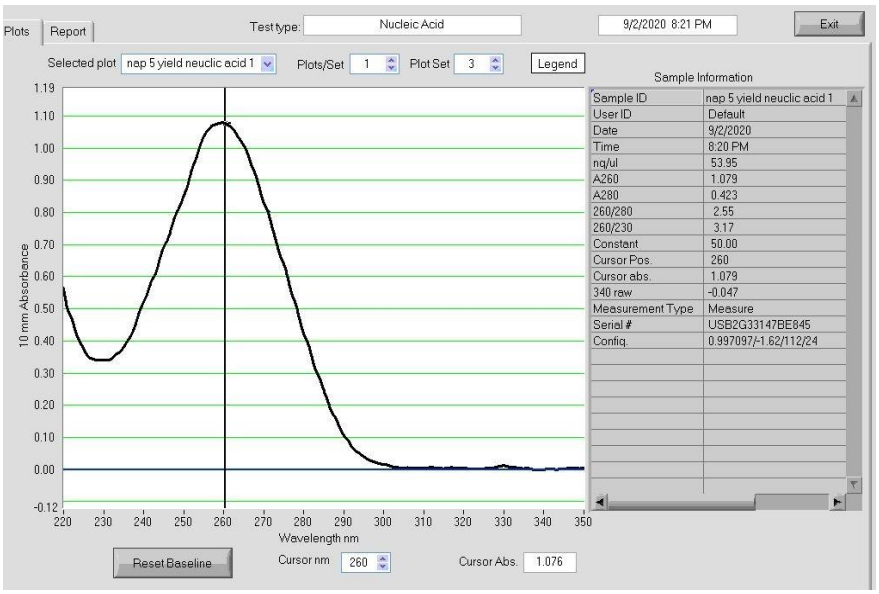

Fig.53Target DNA in 1XPBS

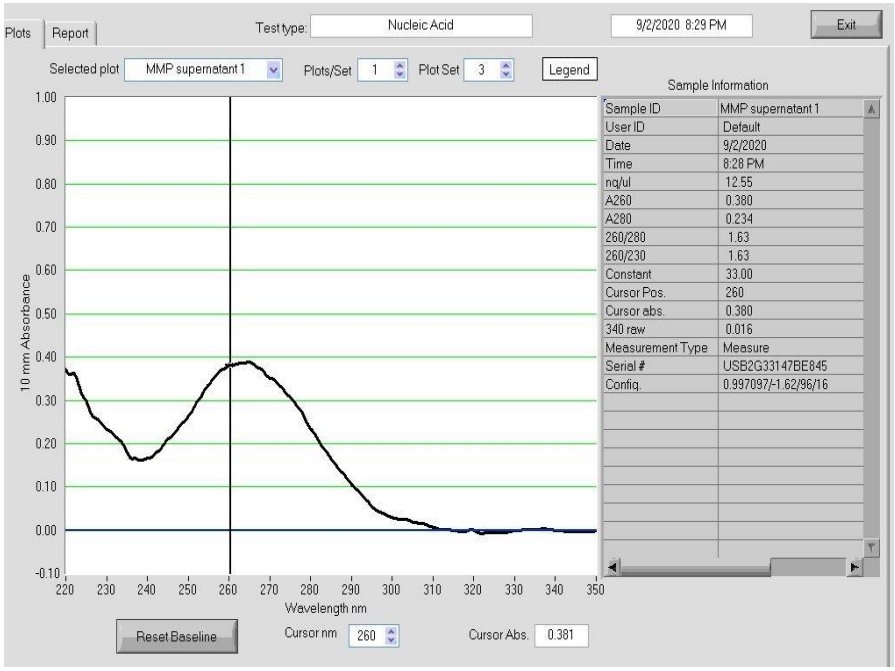

Fig 54Extracted Target DNA in DI

Inference:

Using Beer Lambert's law, we get the concentration of DNA [M] as follows

DNA Type	Absorbance at 260 nm,1nm (obtained from nanodrop)	Concentration [m] Using Beer Lambert's Law
Target DNA in 1XPBS	0.108	3.5E-6
Extracted DNA	0.038	1.26E-6

Table 10 DNA concentration from MMP experiment

The absorbance Extracted DNA showed that the hybridization was Successful. (Target DNA was not thoroughly hybridized and lost in purification steps)

Chapter 5 Conclusion

In this study, a novel approach to obtain satellite nanostructure has been investigated. The effects of temperature, Hybridization buffer concentration, and DNA length on the nanosatellite formation were extensively studied, from which we could achieve the following:

1. Full saturated satellite nanostructures were observed multiple times.
2. A procedure was developed to conjugate Capture and Probe DNA with Au nanoparticles (50nm and 30nm, respectively). This procedure followed a low pH approach. The pH to achieve stable conjugates ranged between 2.3 to 2.5. majority of these conjugates are stable even in 2MNaCl
3. An adequate sample cleaning procedure which included IPA sonication and DI sonication, was established. This cleaning process produced the cleanest Substrate.
4. Uniformity of APTES SAMs layer is tested by varying the parameters such as immersion time for APTES, NaOH concentration, and APTES Volume. We established that we get a uniform monolayer of APTES by using 30 μL of 0.1M NaOH, 10 μL of APTES solution, and 960 μL of ethanol.
5. A Spacer DNA was introduced to get a robust process for the formation of satellite structures. Various parameters like spacer length, DNA length, and DNA/ Spacer ratio were tested to achieve a robust process. From these parameters, a combination of spacer DNA with 18 bases and capture and probe DNA of 48 and 46 bases were consistently forming a nanosatellite structures.
6. A trend that is increasing the DNA length increased P30 nanoparticle attachment to C-50 nanoparticles was established.

7. The issue of P30 nanoparticle detachment from *C*-AuNPs was resolved by introducing a quick IPA dip after stringency washing; the quick IPA dip removed any residual stringency washing buffer and stabilized the nanostructure.
8. A procedure was established to extract and purify the Target DNA using functionalized magnetic microparticles (MMP).

References

1. Pray, L.J.N.E., *Discovery of DNA structure and function: Watson and Crick.* 2008. **1**(1).
2. Sinden, R.R., *DNA structure and function*. 1994: Gulf Professional Publishing.
3. Yin, Y. and X.S.J.A.o.c.r. Zhao, *Kinetics and dynamics of DNA hybridization.* 2011. **44**(11): p. 1172-1181.
4. Herizchi, R., et al., *Current methods for synthesis of gold nanoparticles.* 2016. **44**(2): p. 596-602.
5. Freitas de Freitas, L., et al., *An overview of the synthesis of gold nanoparticles using radiation technologies.* 2018. **8**(11): p. 939.
6. Zhao, P., N. Li, and D.J.C.C.R. Astruc, *State of the art in gold nanoparticle synthesis.* 2013. **257**(3-4): p. 638-665.
7. Dong, J., et al., *Synthesis of precision gold nanoparticles using Turkevich method.* 2020. **37**: p. 224-232.
8. Huang, C.-J., et al., *Electrochemically controlling the size of gold nanoparticles.* 2006. **153**(12): p. D193.
9. Jana, N.R., L. Gearheart, and C.J.J.L. Murphy, *Seeding growth for size control of 5− 40 nm diameter gold nanoparticles.* 2001. **17**(22): p. 6782-6786.
10. Shankar, S.S., et al., *Biological synthesis of triangular gold nanoprisms.* 2004. **3**(7): p. 482-488.
11. Kim, K.-S., D. Demberelnyamba, and H.J.L. Lee, *Size-selective synthesis of gold and platinum nanoparticles using novel thiol-functionalized ionic liquids.* 2004. **20**(3): p. 556-560.
12. Khan, I., K. Saeed, and I.J.A.j.o.c. Khan, *Nanoparticles: Properties, applications and toxicities.* 2019. **12**(7): p. 908-931.
13. Tartaj, P., et al., *Advances in magnetic nanoparticles for biotechnology applications.* 2005. **290**: p. 28-34.
14. An, H. and B.J.B.a. Jin, *Prospects of nanoparticle–DNA binding and its implications in medical biotechnology.* 2012. **30**(6): p. 1721-1732.
15. Madkour, L.H.J.G.D. and Therapeutics, *Ecofriendly green biosynthesized of metallic nanoparticles: bio-reduction mechanism, characterization and pharmaceutical applications in biotechnology industry.* 2018. **3**(1).
16. C Thomas, S., P. Kumar Mishra, and S.J.C.p.d. Talegaonkar, *Ceramic nanoparticles: fabrication methods and applications in drug delivery.* 2015. **21**(42): p. 6165-6188.
17. De Jong, W.H. and P.J.J.I.j.o.n. Borm, *Drug delivery and nanoparticles: applications and hazards.* 2008. **3**(2): p. 133.
18. Khan, A., et al., *Gold nanoparticles: synthesis and applications in drug delivery.* 2014. **13**(7): p. 1169-1177.
19. Khan, I., et al., *Nanobiotechnology and its applications in drug delivery system: a review.* 2015. **9**(6): p. 396-400.
20. Schneider, R., et al., *Lead–germanate glasses: an easy growth process for silver nanoparticles and their promising applications in photonics and catalysis.* 2017. **7**(66): p. 41479-41485.

21. Ang, A.S., et al., *'Photonic Hook'based optomechanical nanoparticle manipulator.* 2018. **8**(1): p. 1-7.
22. Tsangarides, C.P., et al., *Computational modelling and characterisation of nanoparticle-based tuneable photonic crystal sensors.* 2014. **4**(21): p. 10454-10461.
23. Venditti, I.J.M., *Gold nanoparticles in photonic crystals applications: A review.* 2017. **10**(2): p. 97.
24. He, Z., Z. Zhang, and S.J.M.R.E. Bi, *Nanoparticles for organic electronics applications.* 2020. **7**(1): p. 012004.
25. Kanelidis, I. and T.J.B.j.o.n. Kraus, *The role of ligands in coinage-metal nanoparticles for electronics.* 2017. **8**(1): p. 2625-2639.
26. Ko, S.H., et al., *Direct nanoimprinting of metal nanoparticles for nanoscale electronics fabrication.* 2007. **7**(7): p. 1869-1877.
27. Maekawa, K., et al., *Drop-on-demand laser sintering with silver nanoparticles for electronics packaging.* 2012. **2**(5): p. 868-877.
28. Magdassi, S., M. Grouchko, and A.J.M. Kamyshny, *Copper nanoparticles for printed electronics: routes towards achieving oxidation stability.* 2010. **3**(9): p. 4626-4638.
29. Li, B., Y. Du, and S.J.A.c.a. Dong, *DNA based gold nanoparticles colorimetric sensors for sensitive and selective detection of Ag (I) ions.* 2009. **644**(1-2): p. 78-82.
30. Wang, C. and C.J.R.i.A.C. Yu, *Detection of chemical pollutants in water using gold nanoparticles as sensors: a review.* 2013. **32**(1): p. 1-14.
31. Goel, S., F. Chen, and W.J.S. Cai, *Synthesis and biomedical applications of copper sulfide nanoparticles: from sensors to theranostics.* 2014. **10**(4): p. 631-645.
32. Segev-Bar, M. and H.J.A.n. Haick, *Flexible sensors based on nanoparticles.* 2013. **7**(10): p. 8366-8378.
33. Rudramurthy, G.R. and M.K.J.J.J.o.B.I.C. Swamy, *Potential applications of engineered nanoparticles in medicine and biology: An update.* 2018. **23**(8): p. 1185-1204.
34. Dreaden, E.C., et al., *The golden age: gold nanoparticles for biomedicine.* 2012. **41**(7): p. 2740-2779.
35. Giner-Casares, J.J., et al., *Inorganic nanoparticles for biomedicine: where materials scientists meet medical research.* 2016. **19**(1): p. 19-28.
36. Pankhurst, Q., et al., *Progress in applications of magnetic nanoparticles in biomedicine.* 2009. **42**(22): p. 224001.
37. Mirkin, C.A., et al., *A DNA-based method for rationally assembling nanoparticles into macroscopic materials.* 1996. **382**(6592): p. 607-609.
38. Alivisatos, A.P., et al., *Organization of'nanocrystal molecules' using DNA.* 1996. **382**(6592): p. 609-611.
39. Mitchell, G.P., C.A. Mirkin, and R.L.J.J.o.t.A.C.S. Letsinger, *Programmed assembly of DNA functionalized quantum dots.* 1999. **121**(35): p. 8122-8123.
40. Yigit, M.V., et al., *Smart "turn-on" magnetic resonance contrast agents based on aptamer-functionalized superparamagnetic iron oxide nanoparticles.* 2007. **8**(14): p. 1675-1678.

41. Graham, D., et al., *Control of enhanced Raman scattering using a DNA-based assembly process of dye-coded nanoparticles.* 2008. **3**(9): p. 548-551.
42. Lee, J.-S., et al., *Silver nanoparticle− oligonucleotide conjugates based on DNA with triple cyclic disulfide moieties.* 2007. **7**(7): p. 2112-2115.
43. Yang, H., et al., *Engineering target-responsive hydrogels based on aptamer− target interactions.* 2008. **130**(20): p. 6320-6321.
44. Park, S.J., et al., *Directed assembly of periodic materials from protein and oligonucleotide-modified nanoparticle building blocks.* 2001. **40**(15): p. 2909-2912.
45. Hashimoto, K., K. Ito, and Y.J.A.c. Ishimori, *Sequence-specific gene detection with a gold electrode modified with DNA probes and an electrochemically active dye.* 1994. **66**(21): p. 3830-3833.
46. Hegner, M., P. Wagner, and G.J.F.l. Semenza, *Immobilizing DNA on gold via thiol modification for atomic force microscopy imaging in buffer solutions.* 1993. **336**(3): p. 452-456.
47. Storhoff, J.J. and C.A.J.C.R. Mirkin, *Programmed materials synthesis with DNA.* 1999. **99**(7): p. 1849-1862.
48. Zhao, W., M.A. Brook, and Y.J.C. Li, *Design of gold nanoparticle-based colorimetric biosensing assays.* 2008. **9**(15): p. 2363-2371.
49. Rosi, N.L. and C.A.J.C.r. Mirkin, *Nanostructures in biodiagnostics.* 2005. **105**(4): p. 1547-1562.
50. Qian, X., X. Zhou, and S.J.J.o.t.A.C.S. Nie, *Surface-enhanced Raman nanoparticle beacons based on bioconjugated gold nanocrystals and long range plasmonic coupling.* 2008. **130**(45): p. 14934-14935.
51. Giljohann, D.A., et al., *Gold nanoparticles for biology and medicine.* 2010. **49**(19): p. 3280-3294.
52. Zhang, X., et al., *Toward fast and quantitative modification of large gold nanoparticles by thiolated DNA: scaling of nanoscale forces, kinetics, and the need for thiol reduction.* 2013. **117**(30): p. 15677-15684.
53. Storhoff, J.J., et al., *One-pot colorimetric differentiation of polynucleotides with single base imperfections using gold nanoparticle probes.* 1998. **120**(9): p. 1959-1964.
54. Cutler, J.I., E. Auyeung, and C.A.J.J.o.t.A.C.S. Mirkin, *Spherical nucleic acids.* 2012. **134**(3): p. 1376-1391.
55. Zhang, X., M.R. Servos, and J.J.L. Liu, *Surface science of DNA adsorption onto citrate-capped gold nanoparticles.* 2012. **28**(8): p. 3896-3902.
56. Shi, D., et al., *A facile and efficient method to modify gold nanorods with thiolated DNA at a low pH value.* 2013. **49**(25): p. 2533-2535.
57. Barlow, S.M. and R.J.S.s.r. Raval, *Complex organic molecules at metal surfaces: bonding, organisation and chirality.* 2003. **50**(6-8): p. 201-341.
58. Love, J.C., et al., *Self-assembled monolayers of thiolates on metals as a form of nanotechnology.* 2005. **105**(4): p. 1103-1170.
59. Aswal, D., et al., *Self assembled monolayers on silicon for molecular electronics.* 2006. **568**(1-2): p. 84-108.
60. Dong, S., J.J.B. Li, and bioenergetics, *Self-assembled monolayers of thiols on gold electrodes for bioelectrochemistry and biosensors.* 1997. **42**(1): p. 7-13.

61. Sheen, C.W., et al., *A new class of organized self-assembled monolayers: alkane thiols on gallium arsenide (100).* 1992. **114**(4): p. 1514-1515.
62. Vericat, C., et al., *Self-assembled monolayers of thiols and dithiols on gold: new challenges for a well-known system.* 2010. **39**(5): p. 1805-1834.
63. Oh, M.-J., et al., *Preparation of hydrophobic self-assembled monolayers on paper surface with silanes.* 2011. **17**(1): p. 149-153.
64. Smith, M.B., et al., *Study of the packing density and molecular orientation of bimolecular self-assembled monolayers of aromatic and aliphatic organosilanes on silica.* 2007. **23**(2): p. 673-683.
65. Tosatti, S., et al., *Self-assembled monolayers of dodecyl and hydroxy-dodecyl phosphates on both smooth and rough titanium and titanium oxide surfaces.* 2002. **18**(9): p. 3537-3548.
66. Kanta, A., et al., *The formation and stability of self-assembled monolayers of octadecylphosphonic acid on titania.* 2006. **291**(1-3): p. 51-58.
67. Textor, M., et al., *Structural chemistry of self-assembled monolayers of octadecylphosphoric acid on tantalum oxide surfaces.* 2000. **16**(7): p. 3257-3271.
68. Laibinis, P.E., et al., *Comparison of the structures and wetting properties of self-assembled monolayers of n-alkanethiols on the coinage metal surfaces, copper, silver, and gold.* 1991. **113**(19): p. 7152-7167.
69. Gooding, J.J., et al., *Self-assembled monolayers into the 21st century: recent advances and applications.* 2003. **15**(2): p. 81-96.
70. Kim, J., et al., *Investigations of chemical modifications of amino-terminated organic films on silicon substrates and controlled protein immobilization.* 2010. **26**(4): p. 2599-2608.
71. Bishop, A.R., R.G.J.C.O.i.C. Nuzzo, and I. Science, *Self-assembled monolayers: Recent developments and applications.* 1996. **1**(1): p. 127-136.
72. Malel, E., J. Colleran, and D.J.E.a. Mandler, *Studying the localized deposition of Ag nanoparticles on self-assembled monolayers by scanning electrochemical microscopy (SECM).* 2011. **56**(20): p. 6954-6961.
73. Acres, R.G., et al., *Molecular structure of 3-aminopropyltriethoxysilane layers formed on silanol-terminated silicon surfaces.* 2012. **116**(10): p. 6289-6297.
74. Qin, M., et al., *Two methods for glass surface modification and their application in protein immobilization.* 2007. **60**(2): p. 243-249.
75. Chiang, C.-H., et al., *Magic-angle cross-polarization carbon 13 NMR study of aminosilane coupling agents on silica surfaces.* 1982. **86**(1): p. 26-34.
76. Vaidya, A.A. and M.L.J.L. Norton, *DNA attachment chemistry at the flexible silicone elastomer surface: Toward disposable microarrays.* 2004. **20**(25): p. 11100-11107.
77. Vandenberg, E.T., et al., *Structure of 3-aminopropyl triethoxy silane on silicon oxide.* 1991. **147**(1): p. 103-118.
78. Moiseev, L., et al., *DNA conformation on surfaces measured by fluorescence self-interference.* 2006. **103**(8): p. 2623-2628.
79. Zheng, Y., et al., *DNA-directed self-assembly of core-satellite plasmonic nanostructures: A highly sensitive and reproducible near-IR SERS sensor.* 2013. **23**(12): p. 1519-1526.

80. Deal, B.E. and A.J.J.o.a.p. Grove, *General relationship for the thermal oxidation of silicon.* 1965. **36**(12): p. 3770-3778.
81. Pan, P., et al., *The composition and properties of PECVD silicon oxide films.* 1985. **132**(8): p. 2012.
82. da Silva Zambom, L., R.D. Mansano, and A.P.J.M.j. Mousinho, *Low-temperature deposition of silicon oxide and silicon nitride by reactive magnetron sputtering.* 2009. **40**(1): p. 66-69.
83. Irene, E.A., H. Massoud, and E.J.J.o.t.E.S. Tierney, *Silicon oxidation studies: Silicon orientation effects on thermal oxidation.* 1986. **133**(6): p. 1253.
84. Deal, B.E.J.J.o.T.E.S., *The oxidation of silicon in dry oxygen, wet oxygen, and steam.* 1963. **110**(6): p. 527.
85. Vickridge, I., et al., *Growth of SiO2 on SiC by dry thermal oxidation: mechanisms.* 2007. **40**(20): p. 6254.
86. Kao, D.-B., et al., *Two-dimensional thermal oxidation of silicon—I. Experiments.* 1987. **34**(5): p. 1008-1017.
87. Uematsu, M., H. Kageshima, and K.J.C.m.s. Shiraishi, *Microscopic mechanism of thermal silicon oxide growth.* 2002. **24**(1-2): p. 229-234.
88. Bhushan, B., *Encyclopedia of nanotechnology*. 2012: Springer Dordrecht, The Netherlands:.
89. Gosálvez, M.A., I. Zubel, and E. Viinikka, *Wet etching of silicon*, in *Handbook of silicon based MEMS materials and technologies*. 2010, Elsevier. p. 447-480.
90. Knotter, D.M.J.J.o.t.A.C.S., *Etching mechanism of vitreous silicon dioxide in HF-based solutions.* 2000. **122**(18): p. 4345-4351.
91. Tilli, M., et al., *Handbook of silicon based MEMS materials and technologies*. 2020: Elsevier.
92. Zhou, W., et al., *Fundamentals of scanning electron microscopy (SEM)*, in *Scanning microscopy for nanotechnology*. 2006, Springer. p. 1-40.
93. Vernon-Parry, K.J.I.-V.R., *Scanning electron microscopy: an introduction.* 2000. **13**(4): p. 40-44.
94. Joy, D.C. and J.B.J.U. Pawley, *High-resolution scanning electron microscopy.* 1992. **47**(1-3): p. 80-100.
95. Burgess, C., *The basics of spectrophotometric measurement*, in *Techniques and Instrumentation in Analytical Chemistry*. 2007, Elsevier. p. 1-19.
96. Yadav, L., *Ultraviolet (UV) and visible spectroscopy*, in *Organic Spectroscopy*. 2005, Springer. p. 7-51.
97. Abbas, Q.J.J.o.N. and M. Nanotechnology, *Understanding the UV-Vis spectroscopy for nanoparticles.* 2019. **8**(3): p. 1-3.
98. Perkampus, H.-H., *UV-VIS Spectroscopy and its Applications*. 2013: Springer Science & Business Media.
99. Van Den Broeke, J., G. Langergraber, and A.J.S.e. Weingartner, *On-line and in-situ UV/vis spectroscopy for multi-parameter measurements: a brief review.* 2006. **18**(4): p. 15-18.